The effect of ionizing radiation on $^1O_2$ production by Ce6 and TiO_2

NB3000: Bachelor End Project

J.Y.A. Hu

Delft University of Technology

TU Delft

The effect of ionizing radiation on $^1O_2$ production by Ce6 and TiO_2

by

J.Y.A. Hu

Student Name	Student Number
Joey Hu	5071534

Supervisor: Dr. ir. A. G. Denkova,
Daily supervisor: Ir. B. Xu,
Project Duration: February, 2023 - June, 2023
Faculty: Applied Radiation and Isotopes, Reactor Institute Delft

TU Delft

Abstract

Photosensitizers play a key role in photodynamic therapy as a drug that is activated by light. In this thesis, the effect of ionizing radiation on the generation of singlet oxygen when using photosensitizers (Chlorin e6) and photocatalysts (titanium dioxide) was studied.

By using radionuclides and photosensitizers (PS), cells can be killed with reactive oxygen species (ROS) which are produced by PS under influence of radiation that is emitted by radioactive decay. ROS are produced naturally in cells, but an excess of ROS can lead to damage to proteins, nucleic acids, lipids, membranes and organelles, which can lead to activation of cell death processes such as apoptosis. The focus of this thesis is the production of singlet oxygen which is a type of ROS.

Indium-111, lutetium-177 and yttrium-90 which decay by different types of radiation have been used as radiation sources. In this research, the influence of these different radiation sources have been tested on Ce6 and TiO_2 and their ability to produce singlet oxygen.

Results show that Ce6 and TiO_2 have increased production of singlet oxygen when exposed to ionizing radiation. Ce6 generates singlet oxygen when irradiated by both low energy gamma sources and high energy beta-minus radiation, while TiO_2 generates singlet oxygen when irradiated by high energy beta-minus radiation.

Contents

Abstract i

Nomenclature iv

1 Introduction 1

2 Theory 2
2.1 Neoplasms . . . 2
2.2 Radiation . . . 2
2.2.1 Radionuclides . . . 2
2.2.2 Radiation sources . . . 4
2.3 Nuclear Medicine . . . 5
2.4 Radiotherapy . . . 5
2.4.1 Advantages and drawbacks of radiotherapy . . . 5
2.5 Photodynamic Therapy . . . 5
2.5.1 Advantages and drawbacks of PDT . . . 5
2.5.2 Photosensitizers and photocatalysts . . . 6
2.5.3 Reactive Oxygen Species . . . 6
2.5.4 Probe: Singlet Oxygen Sensor Green . . . 7
2.6 Radiolabeling . . . 8

3 Experimental Section 10
3.1 Radiation sources . . . 10
3.2 Materials . . . 10
3.3 Equipment . . . 12
3.3.1 Fluorescence Spectrophotometer . . . 12
3.3.2 Phosphor imager . . . 12
3.3.3 Flatbed scanner . . . 12
3.4 Methods . . . 12
3.4.1 $^1O_2$ detection . . . 12
3.4.2 Precipitation test with indium . . . 13
3.4.3 Chelation experiments . . . 13

4 Results 16
4.1 $^1O_2$ detection . . . 16
4.1.1 Lutetium-177 . . . 16
4.1.2 Indium-111 . . . 18
4.1.3 Yttrium-90 . . . 24

5 Discussion 30
5.1 $^1O_2$ formation . . . 30
5.1.1 Precipitation phenomenon . . . 30
5.1.2 Effect of ionizing radiation on TiO_2 . . . 30
5.1.3 Effect of ionizing radiation on Ce6 and PpIX . . . 30
5.2 Possible photosensitization mechanism . . . 31
5.3 Applicability in medicine . . . 31

6 Conclusion 32
6.1 Effect of ionizing radiation on Ce6 and TiO_2 . . . 32

References 33

A MATLAB code 36

B Chelation results **37**

Nomenclature

Abbreviations

Abbreviation	Definition
Ce6	Chlorin e6
CT	Computed topography
DTPA	Diethylenetriamine pentaacetate
EC	Electron capture
HCl	Hydrogen Chloride
Hf	Hafnium
In	Indium
Lu	Lutetium
PDT	Photodynamic therapy
PE	Polyethylene
PpIX	Protoporphyrin IX
PS	Photosensitizers
RID	Reactor Institute Delft
ROS	Reactive oxygen species
RT	Room Temperature
SOSG	Singlet Oxygen Sensor Green
TiO_2	Titanium dioxide
TLC	thin layer chromatography
Y	Yttrium

Symbols

Symbol	Definition	Unit
A	Activity	[Bq]
c	Concentration	[M]
D	Dose	[Gy]
E	Energy	[eV]
m	Mass	[kg]
n	Number of moles	[mole]
t	Time	[s]
V	Volume	[L]
α	Alpha radiation	
β	Beta radiation	
γ	Gamma radiation	
λ	Decay constant	[s^{-1}]
ρ	Density	[kg/m^3]

1 Introduction

In the Netherlands, 28 percent of deaths in 2022 were caused by malignant neoplasms, or cancer [1]. This makes cancer one of the most leading causes of death. Thus, treating cancer is of utmost importance.

In modern medicine, there is a variety of treatments available to battle malignant neoplasms, including but not limited to: surgery, hyperthermia, chemotherapy, immunotherapy, radiation therapy, hormone therapy and photodynamic therapy. Usually, these types of treatments are not mutually exclusive, but complement each other and are used in a variety of combinations, such as chemotherapy with radiation therapy [2].

In radiotherapy, high-energy radiation from x-rays, gamma rays, neutrons, protons, and other sources are used to kill cancer cells and shrink tumors. Radiation may come from a machine outside the body (external-beam radiation therapy), or it may come from radioactive material placed in the body near cancer cells (internal radiation therapy or brachytherapy) [3].

Internal radiotherapy is a promising treatment. Notwithstanding, one of the limitations is that surrounding tissue may be damaged. Therefore, the use of radiotherapy is limited depending on the location of the targeted tissue. Another treatment method is photodynamic therapy. In photodynamic therapy, a photosensitizer (PS), a drug activated by light, is used to kill cells. Photodynamic therapy is usually used for treatment of specific body parts, local treatment. One of the main drawbacks is that, normally, the activator of the PS is outside the body and cannot pass through more than about 1 centimeter of tissue [4].

These two treatments can be combined and their main drawbacks are less prominent by using photosensitizers together with radionuclides. These can be put into the body and bypass the penetration issue seen in photodynamic therapy and limit the effect of surrounding tissue being damaged.

This thesis will focus on the effect of different sources of ionizing radiation on photosensitizers, such as Chlorin e6 (Ce6) and photocatalysts, such as TiO_2, and their ability of producing singlet oxygen (a reactive oxygen species). The main focus is discovering whether Chlorin e6 (Ce6) and TiO_2 can be activated by ionizing radiation to produce singlet oxygen. The relative amounts of singlet oxygen present after irradiation are measured with fluorescence spectroscopy.

Thus, in this report, we investigate the potential of combining of ionizing radiation with photosensitization to battle cancer. We do this by first discussing relevant theory for this report in chapter 2. Secondly, the experimental setup is explained in chapter 3. Chapter 4 will be a chapter on the results. Following this, in chapter 5 these results will be discussed with possible future endeavors on this particular subject. And finally chapter 6 gives the main conclusions to be drawn from this thesis.

2

Theory

2.1. Neoplasms

A neoplasm is an abnormal mass of tissue that forms when cells grow and divide more than they should or do not die when they should. A neoplasm can be benign, which means it may grow large, but it does not invade, or spread into, other tissues. Malignant neoplasm, or cancer, **can** invade other tissues [5].

2.2. Radiation

Before discussing the applications of radiation, it is best to start with the basics. Essentially, electromagnetic radiation is a form of energy that travels through a medium in the form of waves or particles at the speed of light. This radiation originates from a source [6]. Sources can be natural or man-made. Examples of natural sources are minerals in the ground and stars, such as our sun. Man-made sources of radiation are mainly medical, one example is a computed tomography (CT) scanner [7].

There are different types of radiation. Firstly, there is the spectrum of electromagnetic radiation, which includes radio waves, microwaves, infrared rays, visible light, ultraviolet rays, X rays, gamma rays and the neutrino. Secondly, we have particles which are regarded as radiation when traveling at high velocities, so-called ”matter rays”. Examples of such particles are: electrons, protons and neutrons.

The difference between the two types lies in the fact that, theoretically, the first type does not have any mass at rest, while with the second type rest mass **is** present. However, both types can exhibit particle-like and wavelike behavior at appropriate conditions [8].

Radiation can also be divided into non-ionizing radiation and ionizing radiation.

Non-ionizing radiation has a relatively low energy, its energy is not high enough to detach electrons from atoms or molecules. However, it can produce heat by causing matter to vibrate. Some examples of non-ionizing radiation are: visible light, microwaves and radio waves.

Ionizing radiation has a much higher energy. This radiation can cause electrons to detach, making atoms electrically charged and turn them into ions (thus the term ”ionizing”) [9]. A source of such ionizing radiation can be a radionuclide which will be the only source of radiation considered in this report.

2.2.1. Radionuclides

An element is defined by its atom which is a particle consisting of a nucleus surrounded by an electron cloud. The nucleus is formed by protons and neutrons. The chemical properties of an element are only affected by the number of protons, but neutrons do change the mass of an atom. Atoms with the same number of protons but a different number of neutrons are called isotopes [10].

Only a fraction of all isotopes are stable for an indefinite amount of time. Most isotopes disintegrate spontaneously through a process called radioactive decay. In this process, an unstable (parent) nucleus changes into another (daughter) nucleus (which may be stable or unstable itself) by emitting energy in the form of particles or in the form of certain forms of electromagnetic energy. This energy is usually emitted in the form of α particles, β particles, γ rays and neutrinos (ν). In reality, an α particle

is in fact the nucleus of a helium-4 atom. The β particles may be negatively charged (β^-), or positively charged (β^+) [11].

Unstable isotopes which undergo these radioactive decay processes are called radioactive isotopes, radioisotope, radioactive nuclide or radionuclide which will be the term used in this report [12]. Each radionuclide has a specific rate at which it decays, the half-life, and a specific emission scheme. These will be described for each radionuclide discussed.

Types of radioactivity

As was briefly mentioned above, in radioactive decay, energy is emitted in different forms. The different types of radioactivity are explained in short: alpha decay, beta-minus decay, gamma decay, beta-plus decay and electron capture.

Alpha decay In α decay, an α particle (or $^4_2$He) is ejected from a parent nucleus resulting in a daughter nucleus with two protons and two neutrons less. Alpha particles travel at 5 to 7 percent of the speed of light and are relatively slow and heavy compared with other forms of nuclear radiation. Furthermore, they are highly ionizing, are unable to penetrate very far through matter and are brought to rest by a few centimeters of air or less than a tenth of a millimeter of biological tissue [13].

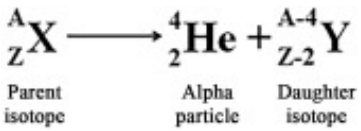

Figure 2.1: α decay: $^4_2$He is ejected from a parent nucleus resulting in a daughter nucleus with two protons and two neutrons less [14].

Beta-minus decay In β^- decay, a neutron decays into a proton, an electron, and an antineutrino. The electron is emitted, producing a daughter nucleus of one higher atomic number and the same mass number. The total charge remains the same, because the number of protons is increased by one in the reaction, but an electron, with negative charge, is also created [11]. Electrons emitted through beta-minus decay are able to penetrate more than alpha particles. The penetration depth depends on the energy of the electron and on the density of the medium it is traveling through. For Y-90, an electron can penetrate up to a depth of 11 millimeters (mm) in soft tissue and in lead up to 1 mm [15].

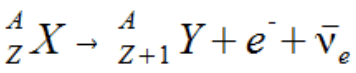

Figure 2.2: β^- decay: An unstable element, X, decays into a new element, Y, via beta minus decay. The new element has one proton more but the atomic mass is unchanged. An electron, and an antineutrino are emitted [16].

Gamma decay In gamma decay, a high energy photon is emitted when there is an excess of energy. The nucleus remains unchanged in atomic number and mass number. Interactions of gamma decay with matter are entirely different from that of charged particles, such as beta particles and alpha particles. The lack of charge eliminates Coulomb interactions and allows gamma rays to be much more penetrating [15].

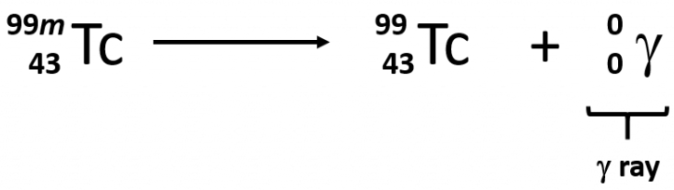

Figure 2.3: γ decay of Technetium-99m [17].

Beta-plus decay In β^+ decay, a positron is created, along with a neutrino. The positron is emitted, producing a daughter nucleus of one atomic number lower and the same mass number [11]. The penetration depth of beta-plus particles are similar to beta-minus particles.

$$ {}^{A}_{Z}X \rightarrow {}^{A}_{Z-1}Y + e^{+} + \nu_e $$

Figure 2.4: β^+ decay: An unstable element, X, decays into a new element, Y, via beta plus decay. The new element has one proton less but the atomic mass is unchanged. A positron, and a neutrino are emitted [16].

Electron capture In Electron capture (EC), an orbital electron is captured by the nucleus. It is similar to β^+ decay in that the nucleus transforms to a daughter of one lower atomic number. It differs in that an orbital electron from its electron cloud is captured by the nucleus. This is followed by emission of X-rays as the orbital vacancy is filled by an electron from the cloud around the nucleus [11].

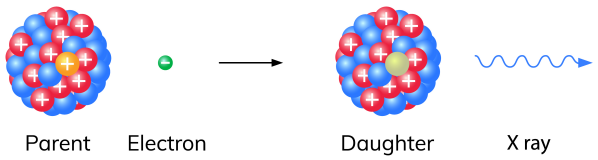

Figure 2.5: Electron capture: The atomic mass of the new element is reduced by one [18].

2.2.2. Radiation sources

In this research, different radiation sources were used. These will be described below.

Yttrium-90

Yttrium (Y) is a rare-earth element of group 3 of the periodic table [19]. Some properties are given in the figure below.
Yttrium has many (unstable) isotopes. For this report, only the radionuclide yttrium-90 was used. Yttrium-90 is a high-energy beta emitter with a half life of 64.1 hours. It decays with a maximum energy of 2.27 MeV $(E_{max} = 2.27MeV)$ and an average energy of 0.93 MeV $(E_{avg} = 0.93MeV)$ [20]. ^{90}Y decays to the stable isotope Zirconium-90 [21].

Indium-111

Indium (In) is a rare metal element of group 13 of the periodic table [22]. Some properties are given in the figure below.

Indium-111 is the only radionuclide of indium that will be discussed in this report. The radionuclide ^{111}In decays by electron capture with a half-life of 2.8 days to cadmium-111 (^{111}Cd). The decay energy of indium-111 is 171 and 245 keV [23].

Lutetium-177
Lutetium (Lu) is a rare-earth metal of the lanthanide series of the periodic table, that is the densest and the highest-melting rare-earth element and the last member of the lanthanide series [24]. Some properties are given in the figure below.
The only radionuclide of Lutetium treated in this report is ^{177}Lu. Lutetium-177 decays by β^- emission and γ emission to Hafnium-177 ($^{177}_{72}$Hf) with a half-life of 6.64 days [25]. It decays with a maximum energy of 0.497 MeV $(E_{max} = 0.497MeV)$.

2.3. Nuclear Medicine

Nuclear medicine uses radioactive material inside the body to see how organs or tissue are functioning (for diagnosis) [26]. An example of this is imaging regions of inflammation using the indium-111 tagged white blood cell scan [27].

2.4. Radiotherapy

In radiotherapy, high-energy radiation from x-rays, gamma rays, neutrons, protons, and other sources are used to kill cancer cells and shrink tumors. Radiation may come from a machine outside the body (external-beam radiation therapy), or it may come from radioactive material placed in the body near cancer cells (internal radiation therapy or brachytherapy) [3].

2.4.1. Advantages and drawbacks of radiotherapy

Radiotherapy has many advantages. The main advantages of radiation therapy are:

- death of a large proportion of cancer cells within the entire tumor;
- ability to shrink tumors;
- relative safety for the patient.

However, there are disadvantages as well. Some major disadvantages are [28]:

- damage to surrounding tissues;
- inability to kill the all cancer cells in tumors;
- inconvenience of radiation therapy (e.g. in some cases it must be delivered daily, 5 days per week, for 1-2 months).

Yttrium-90 is often used in internal radiation therapy.

2.5. Photodynamic Therapy

Photodynamic therapy (PDT) is a type of cancer therapy. In PDT, a photosensitizer, a drug activated by radiation, is used to kill cells. PDT is usually used for treatment of specific body parts, local treatment [4].

2.5.1. Advantages and drawbacks of PDT

Some advantages of PDT are:

- Low side effects;
- Short treatment time;
- Multiple applications at the same location;
- Lower costs.

Nevertheless, PDT also has disadvantages [29]:

- Treatment efficacy dependent on accuracy of tumor light irradiation, light cannot penetrate deeply;
- Tissue oxygenation is crucial for the photodynamic effect, dense tumors can be difficult to treat with PDT;
- Very difficult to treat metastatic cancers with current technology, only irradiated tissue is treated.

2.5.2. Photosensitizers and photocatalysts

A photosensitizer is a drug activated by light. It kills cells by creating cytotoxic molecules which are lethal to cells. These cytotoxic molecules are mainly reactive oxygen species (ROS) [30]. A photocatalyst has a similar role.

The IUPAC gold book has the following definition for photosensitization [31]: "The process by which a photochemical or photophysical alteration occurs in one molecular entity as a result of initial absorption of radiation by another molecular entity called a photosensitizer. In mechanistic photochemistry the term is limited to cases in which the photosensitizer is not consumed in the reaction." Photocatalysis has a similar definition [32]: "Change in the rate of a chemical reaction or its initiation under the action of ultraviolet, visible or infrared radiation in the presence of a substance—the photocatalyst—that absorbs light and is involved in the chemical transformation of the reaction partners."

Thus, photosensitizers and photocatalysts have a similar role in chemical reactions.

2.5.3. Reactive Oxygen Species

Reactive oxygen species, also called oxygen radicals, are unstable molecules which contain oxygen and which easily react with other molecules in a cell [33]. Excess cellular levels of ROS cause damage to proteins, nucleic acids, lipids, membranes and organelles, which can lead to activation of cell death processes such as apoptosis [34]. The most important ROS for this report is singlet oxygen.

Production of ROS

ROS are produced naturally in cells. This happens primarily in the mitochondria. ROS play a crucial role in the proliferation and differentiation in cells either directly or indirectly by modulating the redox status of the cell component and by regulating the vital transcription factors associated with the cellular proliferation and differentiation [35].

The production of ROS by photosensitizers works as follows: illumination transfers energy from light to molecular oxygen, to generate reactive oxygen species (ROS), such as singlet oxygen [36].

In more detail, the ground-state photosensitizer (S_0) is excited to a high-energy state after absorbing excitation photons (Figure 2.6). The energy in this high-energy state can dissipate through various methods, intersystem crossing (ISC) being the most important for the generation of ROS. ISC converts excited, singlet-state molecules into a triplet state, which is a metastable electronic state and would dissipate its energy via phosphorescence or photochemical reactions. Triplet state molecules have a much longer lifetime (microseconds) compared to singlet state molecules (nanoseconds). This could mean more efficient and more energy-transferring collisions.

Generation of ROS could take place by two hypothetical types of photochemical processes (Figure 2.6). For simplicity and because type II is thought to be the more important for most photosensitizers, only the Type II process is considered. It is mechanistically simpler than the Type I process as energy is directly transferred from the excited triplet molecule to a ground-state triplet oxygen, resulting in highly reactive singlet oxygen ($^1O_2$) [37].

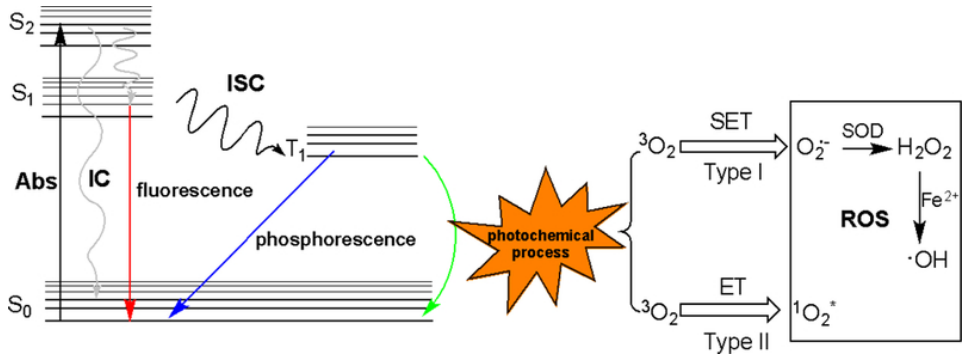

Figure 2.6: Jablonski diagram and mechanisms for photosensitizer-induced ROS generation. Photosensitizers in the ground state are excited to a high-energy singlet state, which could subsequently be converted into a triplet state via ISC. This triplet state may further undergo photochemical reactions via either a type I or a type II process to generate ROS. (Abs, absorption; IC, internal conversion; ISC, intersystem crossing; SET, single electron transfer; ET, energy transfer; SOD, superoxide dismutase) [37].

ROS production by TiO_2 is somewhat different. TiO_2 is a semiconductor. Semiconductors have a valence band containing electrons, and a conduction band which is free of these charged particles. The difference in energy between these two bands is called the energy gap (ΔE) and indicates how much energy is required to excite an electron. The band gap energy is 3.1 eV for TiO_2. An electron moves from the valence band to the conduction band when the energy absorbed exceeds the gap energy. This leaves behind a positive hole, a vacancy in the valence band. This also results in an exciton. This exciton exhibits characteristic redox properties. Both of the charged particles from the electron-hole pair are charge carriers. These charge carries can move up to the surface of the atom. On the surface adsorbed molecules are present. When charge carries move to the surface, they can interact with the adsorbed molecules. This interaction could cause the formation of ROS. Another mechanism which can result in the formation of ROS is the decay of an exciton. Herein, the recombination of an electron-hole pair occurs in a process called radiative recombination. During this, a photon is emitted in response to the excess energy. This can cause the ground state of oxygen to be excited, which could in turn cause the formation of singlet oxygen [38].

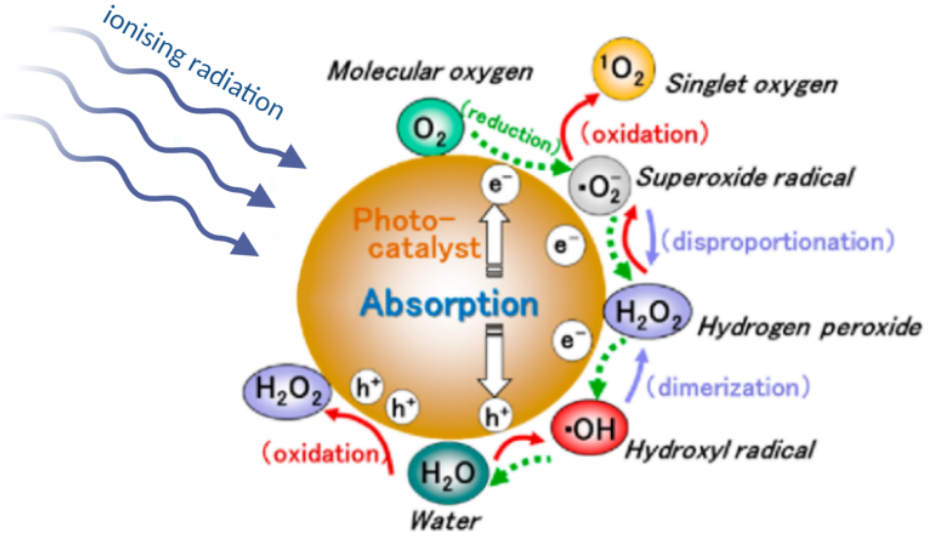

Figure 2.7: Possible mechanisms for Reactive Oxygen Species formation at the surfaces of TiO2 [39].

2.5.4. Probe: Singlet Oxygen Sensor Green

The main ROS used for this study is singlet oxygen. To detect singlet oxygen, the probe Singlet Oxygen Sensor Green **(SOSG)** is used. SOSG emits green fluorescence in presence of singlet oxygen (excitation/emission maxima approx. 504/525nm) [40]. The SOSG dyad has two parts: a trapping moiety and a fluorophore. The trapping moiety (on the right of the molecule) which is an electron donor, quenches the luminescence of the fluorophore by photo-induced electron transfer (PET). When $^1O_2$ is present, the trapping moiety will react with $^1O_2$ and form an endoperoxide anthracene moiety, which has a lower energy for the highest occupied molecular orbital than that of the fluorophore. This leads to the removal of the quenching ability of the trapping moiety which in turn leads to fluorescence emission of the fluorophore under light excitation with a peak at around 530 nm [41].

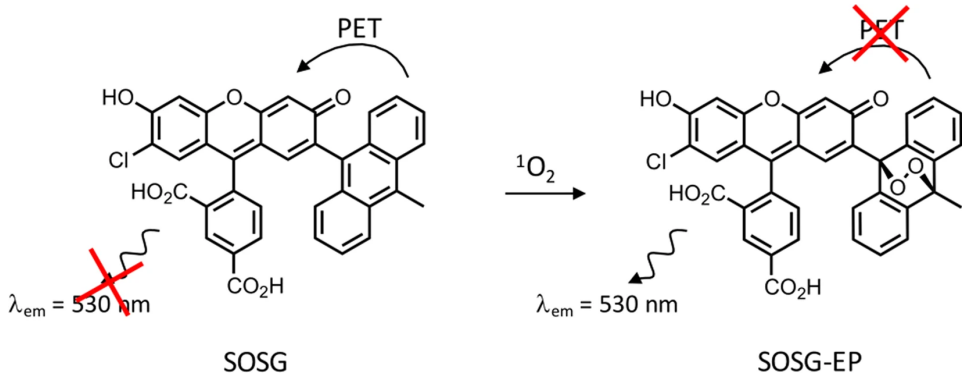

Figure 2.8: Chemical structure of SOSG and the formation of SOSG-EP upon interaction with $^1O_2$, leading to activation of fluorescence output [42].

2.6. Radiolabeling

Radiolabeling is a process that is frequently used in medicine, drug research and development, and environmental case studies. Using this process, researchers can track the movement or breakdown of target molecules. In simple terms, in radiolabeling, we "label" molecules with radioactive isotopes [43].

In this thesis, radiolabeling is making a complex between a radionuclide and a chelator to form a chelated radionuclide. For this research it is important to keep lutetium-177 and indium-111 in solution, this is done by complexation with a chelating agent, DTPA. Complexation with DTPA is done by formation of bonds between a DTPA and a metal ion [44].

Diethylenetriamine pentaacetate (DTPA)

DTPA is a chelating agent or chelator that has been used to treat internal contamination and to remove radioactive isotopes from the body [45]. It has been mainly used for americium, plutonium and curium, but it should also work for other metals. Each COO- group and N-center serves a center for chelation. The compound is not cell membrane permeable [46]. The chemical structure of DTPA and DTPA-indium is shown below.

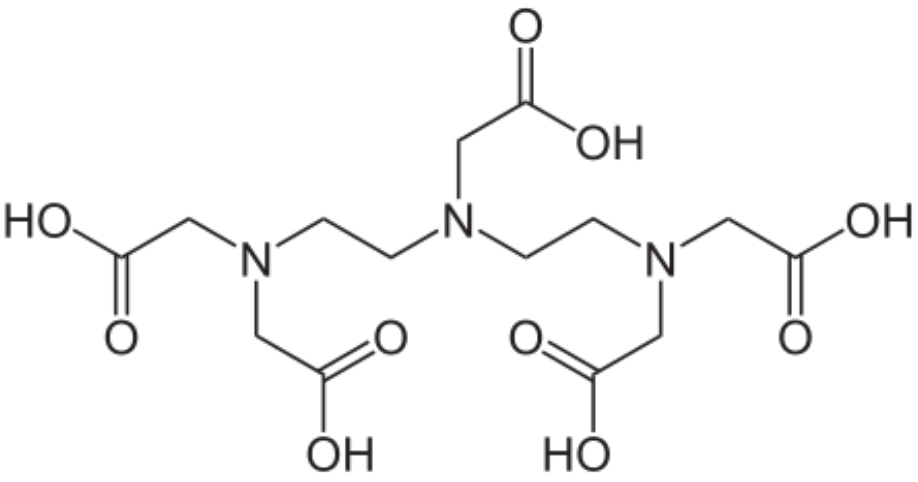

Figure 2.9: Chemical structure of DTPA [47].

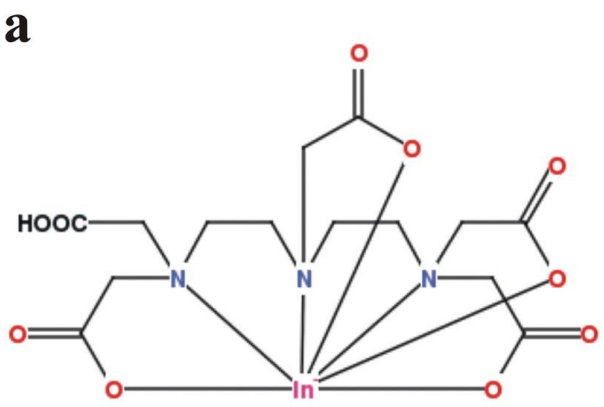

Figure 2.10: ^{111}In-DTPA [48].

3

Experimental Section

This chapter describes the experimental section of this report. First, the equipment and other materials are described, followed by the experimental setups.

3.1. Radiation sources

The radiation sources used in this report were:

- **Lutetium-177:** Lutetium-177 was obtained from the Erasmus Medical Center. Lu-177 was dissolved into a 0.01 M hydrogen chloride (HCl) solution. When it was not used for experiments, the solution was kept in a plastic vial stored in a lead container. The used activities were 0.5 MBq, 0.1 MBq and 0.05 MBq. The specific activity of ^{177}Lu is 0.5 GBq/μg.
- **Indium-111:** Indium-111 was obtained from the Erasmus Medical Center. In-111 was dissolved into a 0.01 M hydrogen chloride (HCl) solution. When it was not used for experiments, the solution was kept in a plastic vial stored in a lead container. Only an activity of 0.4 MBq was used. The specific activity of ^{111}In is 15.5 GBq/μg.
- **Yttrium-90:** Yttrium-90 foils were obtained from Alfa Aesar. These foils were sealed in polyethylene (PE) films and packed in PE-rabbits. These foils were then neutron activated in the BP3 facility of the Reactor Institute Delft (RID). After activation, a foil is stored in a perspex box. The used activities were 12.3 MBq, 34.2 MBq, 96.5 MBq and 157 MBq.

Before experiments, the activity of each radiation source was measured using a dose calibrator from Comecer, the VDC-603.

3.2. Materials

Photosensitizers and photocatalysts

- **TiO$_2$:** TiO$_2$ was obtained from Deutsche Gold- und Silber Scheideanstalt (Degussa). Titanium(IV)oxide P25 was available in powder form. The nanopowder consisted out of a mixture of 85 percent rutile and 15 percent anatase. The average particle size was 20 nm, with a purity of 99.9 percent. For every experiment that involved TiO$_2$, a 0.5 g/L TiO$_2$ solution was made. This was done by first weighing the mass needed and putting that in a glass vial, then MilliQ water was added. The vial was then sealed with aluminum foil to block ambient light. The vial was then sonicated for 30 min.
- **Chlorin e6:** Ce6 was dissolved into Phosphate-buffered saline (PBS) solvent. It was available in a stock solution of 2.5 mg/mL. For every experiment that involved Ce6, a 6 μg/mL solution was made. This was done by putting MilliQ water in a glass vial and adding Ce6 stock solution to the water. The vial was then sealed with aluminum foil to block ambient light. This was shortly sonicated for 10 seconds.
- **Protoporphyrin IX:** PpIX was available in powder form. For PpIX experiments, a μg/mL concentration was chosen. This was done by first weighing the mass needed and putting that in a glass vial, then MilliQ water was added. The vial was then sealed with aluminum foil to block ambient light. The vial was then sonicated for 30 min.

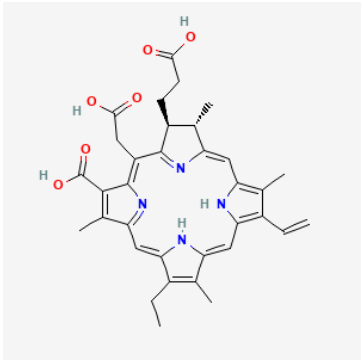

Figure 3.1: Chemical structure of Ce6 [49].

SOSG
SOSG was obtained from Thermo Fisher Scientific Incorporated. The SOSG reagent was provided specially packaged in sets of 10 vials, each containing 100 μg. Before use, 33 μL of pure methanol was added to a vial. This results in a stock solution with a concentration of 5 mM. For the experiments it was chosen to use a concentration of 10 μM. To acquire this desired concentration, SOSG was diluted with water.

DTPA
Diethylenetriamine pentaacetate was available in free acid form making it "diethylenetriamine pentaacetic acid". It was obtained from Fluka. DTPA solutions were made in different concentrations: 0.01 μM, 0.1 μM and 1 μM. These solutions were made by weighing the required mass according to formula 3.1 below.

$$m = c \cdot V \cdot M \tag{3.1}$$

where

- m = mass;
- c = concentration;
- V = volume;
- M_r = molar mass.

After weighing the required mass, it was put into a 10 mL plastic tube. Then, one of two solvents were added. The first one was a 10 mL of sodium acetate solvent (CH_3COONa) with pH = 5.6. This solvent was made by mixing 91 mL 0.2 M sodium acetate (NaOAc) with 9.0 mL 0.2 M acetic acid (HOAc) [50]. The second one was a 10 mL 0.5 M sodium bicarbonate ($NaHCO_3$) solvent with pH = 7.7. This solvent was made by adding MilliQ water to 2.1 g of sodium bicarbonate until the total volume of this solution was 50 mL. To bring the pH down to 7.7, 0.5 M HCl was added to the solution until the pH approximately reached 7.0.

To acquire the required concentrations, DTPA solutions with higher concentrations were diluted with the same solvent used before until the desired concentrations were available.

Other chemicals
- Ammonium acetate was obtained from Sigma-Aldrich;
- Hydrochloric acid was obtained from Honeywell;
- Indium(III)Chloride was obtained from Sigma-Aldrich;
- Methanol was obtained from Honeywell;
- Sodium acetate Anhydrous was obtained from Sigma-Aldrich;
- Sodium bicarbonate was obtained from J.T. Baker Chemicals B.V..

3.3. Equipment

3.3.1. Fluorescence Spectrophotometer

The Cary Eclipse Fluorescence Spectrophotometer from Agilent Technologies (MY16240001) was used to analyze samples. The emission settings for the analysis are given in the table below. For the results, the maximum peak intensity was collected.

Excitation wavelength	504 nm
Start	510 nm
Stop	600 nm
Excitation slit	5.00 nm
Emission slit	5.00 nm

3.3.2. Phosphor imager

For analysis of chelation results, thin layer chromatography was used. A drop of the analyzed solution was put onto TLC paper (iTLC-SG-Glass microfiber chromatography paper impregnated with silica gel from Agilent Technologies). After the TLC process, this paper was put into an exposure cassette with a phosphor screen for ten to fifteen minutes. Then screen was scanned using the Typhoon Trio Phosphor imager from Amersham.

3.3.3. Flatbed scanner

Dose rates for yttrium-90 foils were determined using the Epson Perfection V700 Photo flatbed scanner.

3.4. Methods

3.4.1. $^1\mathbf{O}_2$ detection

Note: the preparation method for SOSG, TiO_2, Ce6 and PpIX were described under section 3.2.

Sample preparation

All samples were prepared by first making batches of SOSG, TiO_2 and Ce6 in glass vials, then for each individual sample a black microcentrifuge tube was taken and filled with water, SOSG, TiO_2, Ce6 and/or PpIX. Black microcentrifuge tubes were used to block out ambient light. Then the samples in the tubes were mixed for certain time periods (ranging from 1 hour to 24 hours) at RT with a Grant-Bio PHMT thermo-shaker. Irradiation was done by either adding ^{177}Lu or ^{111}In radionuclides, or putting samples in a well plate on an ^{90}Y foil.

For TiO_2 samples an extra step was needed before analysis. Since TiO_2 is non-water-soluble, the samples containing TiO_2 were cloudy. To get a proper measurement, TiO_2 needed to be removed from the solution after mixing. This was done by centrifuging at 9,000 rpm for 30 min. This action leaves the nanoparticles at the bottom of the vial, making it easier to pipette only the clear supernatant of the samples.

All samples were then removed from the tubes and put into cuvettes for measurement and analyzed with the spectrophotometer described in the materials.

Lutetium-177 experiments

Following the sample preparation, for the ^{177}Lu experiments, two kinds of samples were prepared: a group containing 0.5 mL pure MilliQ water + 0.5 mL SOSG solution with or without ^{177}Lu (ranging from 0.05 MBq to 0.5 MBq) and a group containing 0.5 mL of the TiO_2 solution + 0.5 mL SOSG solution with or without ^{177}Lu (ranging from 0.05 MBq to 0.5 MBq).

Indium-111 experiments

Following the sample preparation, for the ^{111}In experiments, three kinds of samples were prepared: a group containing 0.6 mL pure MilliQ water + 0.5 mL SOSG solution with or without ^{111}In (A = 0.4 MBq), a group containing 0.6 mL pure Ce6 solution + 0.5 mL SOSG solution with or without ^{111}In (A = 0.4 MBq) and a group containing 0.6 mL of the TiO_2 solution + 0.5 mL SOSG solution with or without ^{111}In (A = 0.4 MBq). *Note: it was decided to increase the volume. In the ^{177}Lu experiments, the experience was that (especially with the TiO_2 samples), not enough volume could be extracted to fill the cuvettes sufficiently.*

Indium-111 with DTPA experiments

For ^{111}In-DTPA experiments, an extra step is added before sample preparation. Indium-111 (A = 0.1 MBq) dissolved in 0.01 M HCl was mixed with a 10 μM DTPA solution. The chosen DTPA solvent was the 10 mL 0.5 M sodium bicarbonate ($NaHCO_3$) solvent with pH = 7.7.

Following the sample preparation, for the ^{111}In-DTPA experiments, three kinds of samples were prepared: a group containing 0.6 mL pure MilliQ water + 0.5 mL SOSG solution with or without ^{111}In-DTPA (A = 0.4 MBq), a group containing 0.6 mL pure Ce6 solution + 0.5 mL SOSG solution with or without ^{111}In-DTPA (A = 0.4 MBq) and a group containing 0.6 mL of the TiO_2 solution + 0.5 mL SOSG solution with or without ^{111}In-DTPA (A = 0.4 MBq).

Yttrium-90 experiments

Different ^{90}Y foils (with activities varying from 12.3 MBq to 157 MBq) were used in these experiments. The setup of a typical ^{90}Y experiment was as follows: firstly, initial dose rates and activity of the ^{90}Y foil were determined. Then, water, SOSG, TiO_2, Ce6 and/or PpIX samples were prepared. These samples were put into a well plate (48 wells). This plate was placed on a ^{90}Y foil that was sealed in a polyethylene (PE) bag. The samples on the well plate should overlap with the area of the foil so that every sample is irradiated. Then the samples were analyzed together with control samples that were not irradiated.

Determining dose rates The initial dose rates of the yttrium-90 foil were determined by measuring GAFchromic™ EBT3 films. The GAFchromic EBT3 film has an initial color of light green and will turn darker while being exposed to radiation. The amount of absorbed dose determines the color of the film, an increase of dose results in a darker film [51]. FIJI/ImageJ software were used to determine the degree of darkening of the films. [52]. An example of this is shown below.

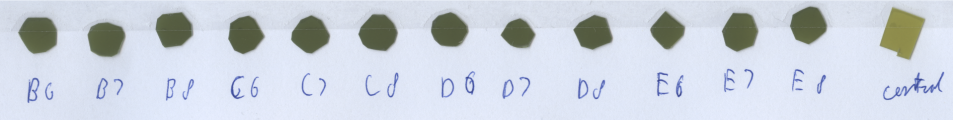

Figure 3.2: a GAFchromic™ EBT3 film after exposure to yttrium-90

Sample preparation Following the sample preparation, for the ^{90}Y experiments, four kinds of samples were prepared: a group containing 0.25 mL pure MilliQ water + 0.25 mL SOSG solution, a group containing 0.25 mL pure Ce6 solution + 0.25 mL SOSG solution, a group containing 0.25 mL of the TiO_2 solution + 0.25 mL SOSG solution and group containing 0.25 mL of the PpiX solution + 0.25 mL SOSG solution. Smaller volumes were chosen, because one well can contain only 0.5 mL.

3.4.2. Precipitation test with indium

Following the sample preparation, for the precipitation with indium experiment, two kinds of samples were prepared: a group containing 0.6 mL pure MilliQ water + 0.5 mL SOSG solution with or without 10 μL 0.5 M indium(III)chloride ($InCl_3$) dissolved in 0.01 M HCl and a group containing 0.6 mL of the TiO_2 solution + 0.5 mL SOSG solution with or without 10 μL 0.5 M $InCl_3$.

3.4.3. Chelation experiments

As will be discussed in more detail in the results section, chelation experiments were needed. To acquire the best radiolabeling efficiency, different experiments with different parameters were performed.

For every chelation experiment the following procedure was followed: 0.1 MBq of ^{111}In dissolved in 0.01 M HCl was mixed with DTPA solutions of concentrations varying from 0.01 μM to 1.0 μM. Since making small concentrations, such as 0.01 μM DTPA solution, directly requires a very small mass, a 10 mM DTPA stock solution was made. This was then diluted to achieve the desired DTPA solution. Next, ^{111}In was mixed with DTPA for time periods varying from 30 minutes to three hours at a speed of 1400 rpm on the thermo-shaker. After mixing, one drop of each sample was dropped onto a TLC paper. After this drop had dried up, the TLC paper was put into a mobile phase.

There were two mobile phases used. The first one was a 0.5 M sodium citrate solution with pH = 5.5. The separation for this mobile phase was as following: chelated Indium-111 was left at the spot where the drop was applied to the paper, free Indium-111 that was not chelated followed the migration of the mobile phase. The second one was an ammonium acetate ($NH_4CH_3CO_2$) solution with pH = 7.7. This solution was made by adding 9 mL MilliQ water and 9 mL pure methanol to 1g of ammonium acetate. The separation was different from the sodium citrate mobile phase, and was as following: free indium-111 that was not chelated remained at the spot where the drop was placed, the ^{111}In-DTPA complex followed the migration of the mobile phase [53].

When the mobile phase almost reached the top of the paper, the paper was taken out of the mobile phase and was left to dry. When the paper was dry, the paper was left inside a box on a phosphor screen for ten to fifteen minutes. Finally, the phosphor screen was scanned using the phosphor imager.

First test

For the first attempt to chelate ^{111}In with DTPA, 0.1 MBq of ^{111}In dissolved in 0.01 M HCl was mixed with 0.01 μM DTPA. The number of moles (n) needed can be calculated using the following formula:

$$n = \frac{A}{\lambda \cdot N_A} = \frac{A}{\frac{ln(2)}{t_{\frac{1}{2}}} \cdot N_A} \tag{3.2}$$

where

- A= activity;
- λ = decay constant;
- $t_{\frac{1}{2}}$ = half-life of Indium-111;
- N_A= Avogrado's number.

The volume of DTPA needed can be calculated using:

$$V = \frac{n}{c} \tag{3.3}$$

where

- n = number of moles;
- c = concentration.

To get a 1:1 mole ratio between Indium-111 and DTPA, the volume of DTPA is 5.824 μL. For this experiment, different ratios between ^{111}In and DTPA were used. These are given in the following table:

Ratio ^{111}In:DTPA	Volume of DTPA
1:1	5.82 μL
1:10	58.2 μL
1:40	233 μL
1:80	466 μL
1:160	932 μL

DTPA was dissolved into 10 mL of sodium acetate solvent (CH_3COONa) with pH = 5.6.

Different solvent, mobile phase and DTPA concentration

For this experiment, 0.1 MBq ^{111}In dissolved in 0.01 M HCl was mixed with a 0.1 μM DTPA solution. For this experiment different ratios between ^{111}In and DTPA were used. These are given in the following table:

Ratio ^{111}In:DTPA	Volume of DTPA
1:10	5.82 μL
1:40	23.3 μL
1:80	46.6 μL

DTPA was dissolved into 10 mL of 0.5 M sodium bicarbonate ($NaHCO_3$) solvent.

Different pH

In a follow-up experiment, the solvent for DTPA of the **first test** (sodium acetate pH = 5.6) was used. All other parameters and procedures (DTPA concentration, shaking time, indium-111 activity, etc.) were the same as the experimental setup mentioned in the section above.

Different mixing time periods

To try and optimize the radiolabeling of ^{111}In with DTPA, different time periods of mixing were performed. For this experiment, 0.1 MBq ^{111}In dissolved in 0.01 M HCl was mixed with a 0.1 μM DTPA solution. DTPA was dissolved into 10 mL of 0.5 M sodium bicarbonate ($NaHCO_3$) solvent.

Higher DTPA concentration: 1.0 μM

To get a higher radiolabeling percentage, ^{111}In was mixed with a solution that had a higher DTPA concentration.

For this experiment, 0.1 MBq ^{111}In dissolved in 0.01 M HCl was mixed with a 1.0 μM DTPA solution. Different ratios were used here, 1:10, 1:100 and 1:1000. DTPA was dissolved into 10 mL of 0.5 M sodium bicarbonate ($NaHCO_3$) solvent.

Testing free indium and indium-DTPA

During sample preparation, $5.824 \cdot 10^{-14}$ moles of indium dissolved in 0.01 M HCl was mixed with a 0.1 μM DTPA solution. Only the 1:100 ration was used here. DTPA was dissolved into 10 mL of 0.5 M sodium bicarbonate ($NaHCO_3$) solvent.

For this experiment, three samples were prepared:

- **sample 1:** 0.6 mL pure MilliQ water + 0.5 mL SOSG solution;
- **sample 2:** 0.6 mL pure MilliQ water + 0.5 mL SOSG solution + 58 μL of 1 nM indium(III)chloride ($InCl_3$) dissolved in 0.01 M HCl.
- **sample 3:** 0.6 mL pure MilliQ water + 0.5 mL SOSG solution + $5.824 \cdot 10^{-14}$ moles of indium complexed with 0.1 μM DTPA.

4

Results

The results that involve the detection of singlet oxygen are shown in this chapter. All results are graphically represented using MATLAB [54]. The code used is given in the appendix.

4.1. $^1\mathbf{O}_2$ detection

The goal of these experiments was to study the effect of ionizing radiation on the generation of singlet oxygen when using photosensitizers (Ce6 and PpIX) and photocatalysts (TiO_2). Using fluorescence spectroscopy, the relative amounts of $^1O_2$ were measured. The output is given in terms of the intensity in arbitrary units (a.u.). Firstly, results from ^{177}Lu experiments will be treated. Followed by the results of the ^{111}In experiments. Finally, the last subsection treats the results of the ^{90}Y experiments.

4.1.1. Lutetium-177

In these experiments, ^{177}Lu was used as the radiation source and mixed with water and TiO_2 solutions. Figure 4.1 shows the fluorescent signal detected from SOSG for samples with and without lutetium-177 and for different radiation times.

Only one sample of each kind was prepared. Figure 4.1 shows the maximum peak intensity plotted. This figure shows that samples that contain the ^{177}Lu radionuclides with time periods 2h and 4h produce less signal intensity compared to samples without radionuclides with the same time periods.

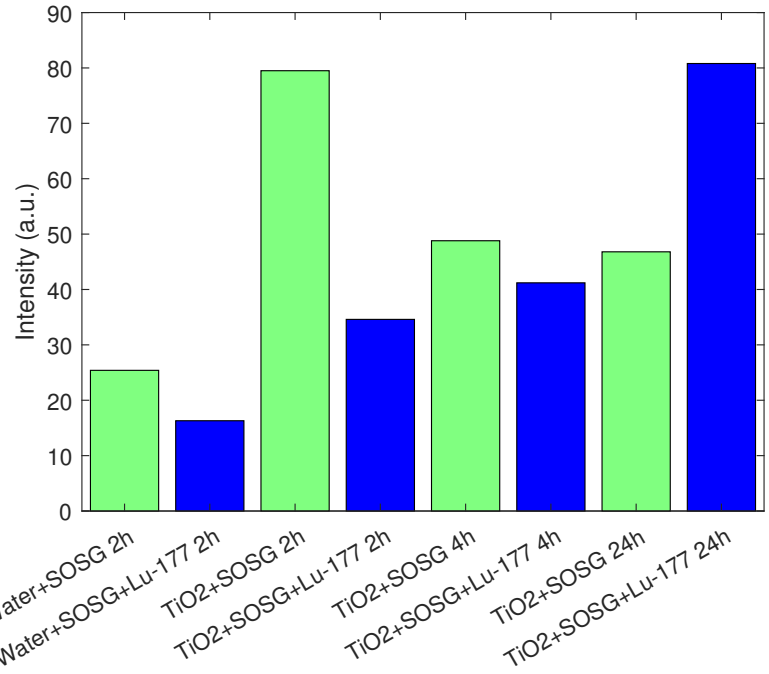

Figure 4.1: The fluorescence of SOSG for samples containing MilliQ water and TiO_2 (0.5 g/L) in the presence and absence of ^{177}Lu for different radiation times. n=1

This result was unexpected. Thus, to check whether the results were correct, another experiment was conducted with lower activities. Figures 4.2 shows the fluorescent signal detected from SOSG for samples with and without lutetium-177 and for 2h of radiation time. Figure 4.3 shows the same but for 24h of radiation time.

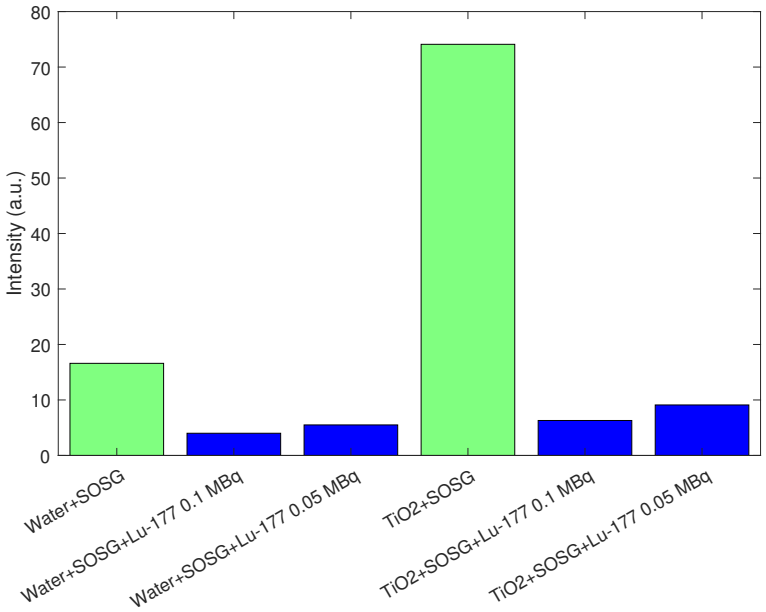

Figure 4.2: The fluorescence of SOSG for samples containing MilliQ water and TiO_2 (0.5 g/L) in the presence and absence of ^{177}Lu for 2h of radiation time. n=1

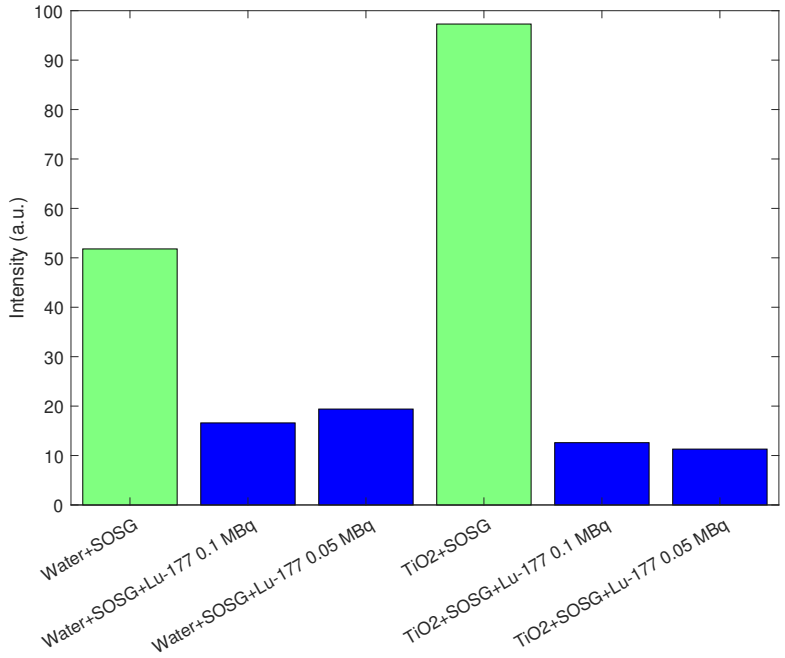

Figure 4.3: The fluorescence of SOSG for samples containing MilliQ water and TiO_2 (0.5 g/L) in the presence and absence of ^{177}Lu for 24h of radiation time. n=1

In figures 4.2 and 4.3, it was shown that adding ^{177}Lu radionuclides resulted in a decrease in signal intensity.

4.1.2. Indium-111

In these experiments, ^{111}In was used as the radiation source and mixed with water and TiO_2 solutions. Figure 4.4 shows the fluorescent signal detected from SOSG for samples with and without indium-111 and for 2h of radiation time. Figure 4.5 shows the fluorescent signal detected from SOSG for samples with and without indium-111 and for 24h of radiation time. Figure 4.4 and figure 4.5 show the maximum peak intensities of each sample. This figure shows that samples that contained the ^{111}In radionuclides had less signal intensity compared to samples without radionuclides.

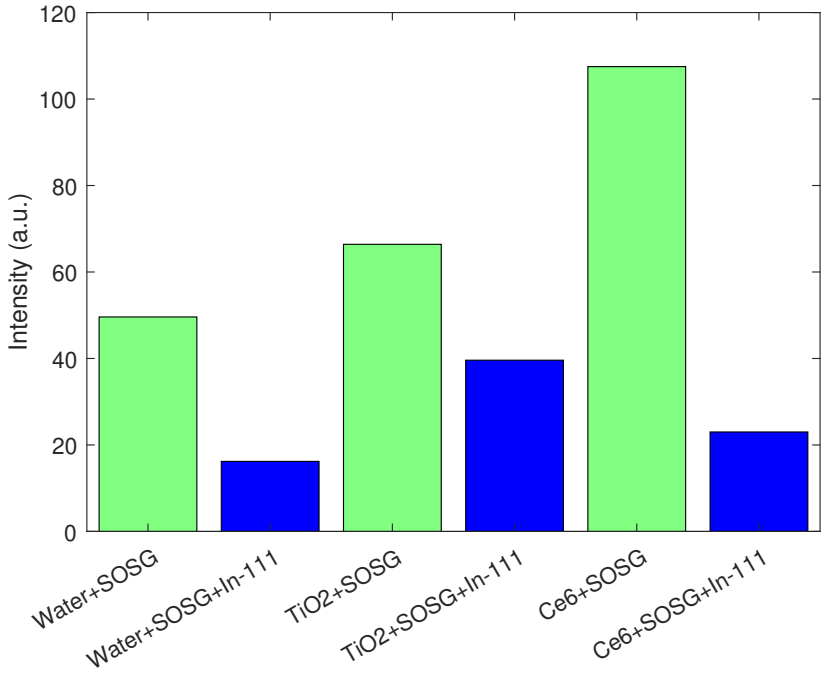

Figure 4.4: The fluorescence of SOSG for samples containing MilliQ water, TiO_2 (0.5 g/L) and Ce6 (6 μg/mL) in the presence and absence of ^{111}In for 2h of radiation time. n=1

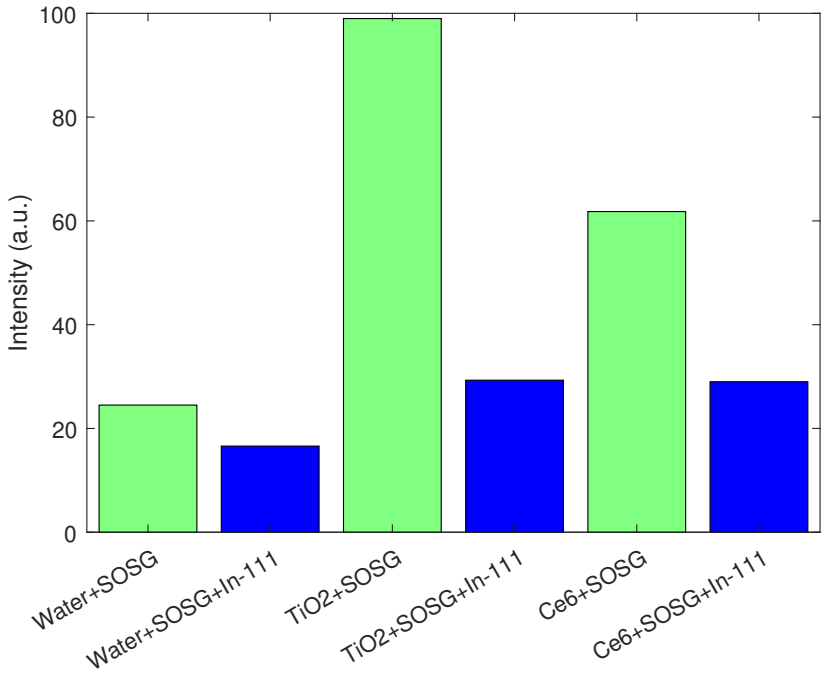

Figure 4.5: The fluorescence of SOSG for samples containing MilliQ water, TiO_2 (0.5 g/L) and Ce6 (6 μg/mL) in the presence and absence of ^{111}In for 24h of radiation time. n=1

Precipitation

The results of the indium-111 experiments are similar to the results of the lutetium-177 experiments. The similarity lies in the fact that, when radionuclides are added, the signal intensity decreases, whereas an increase is expected. This could be due to the precipitation of both indium and lutetium which would

decrease the SOSG signal. To bypass this, it was decided to chelate indium with DTPA. To determine whether precipitation caused the decrease of fluorescence intensity, non-radioactive indium was tested for

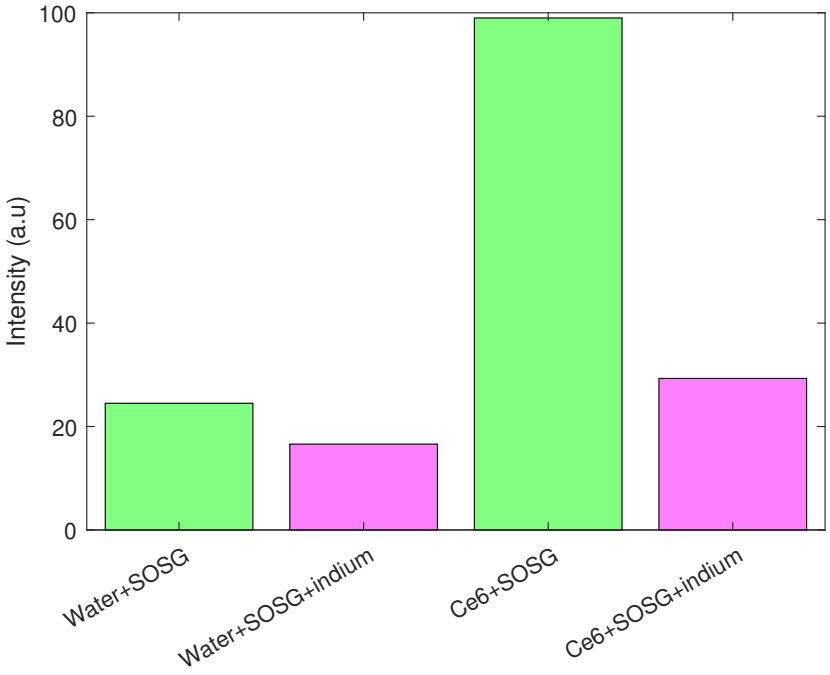

Figure 4.6: The fluorescence of SOSG for samples containing MilliQ water and Ce6 (6 μg/mL) in the presence and absence of indium for 24h of radiation time. n=1

Figure 4.6 confirms that it is the indium itself that causes a decrease in signal intensity. Supposedly, chelating indium with DTPA solves the issue of precipitation. To examine whether this is true, three samples with and without DTPA and only containing SOSG were tested.

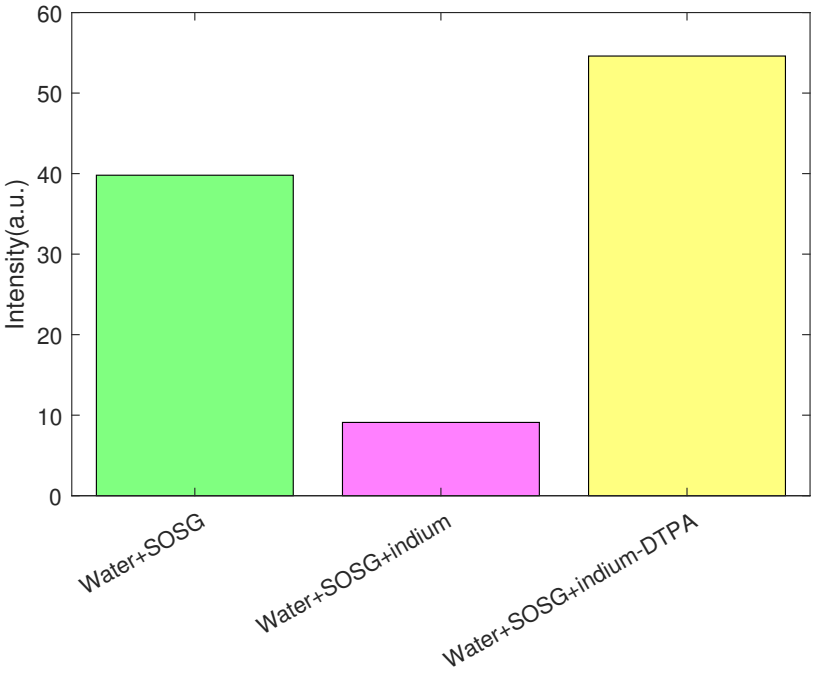

Figure 4.7: The fluorescence of SOSG for samples containing MilliQ water in the presence and absence of indium and indium-DTPA for 2h of radiation time. n=1

Figure 4.7 shows that chelation with DTPA does lead to solving the precipitation issue. This results in a larger fluorescence signal intensity.

^{111}In-DTPA experiments

It is clear that indium-111 should be chelated with DTPA before interaction with SOSG. The same type of experiments as before were performed but now with ^{111}In-DTPA instead of only ^{111}In.

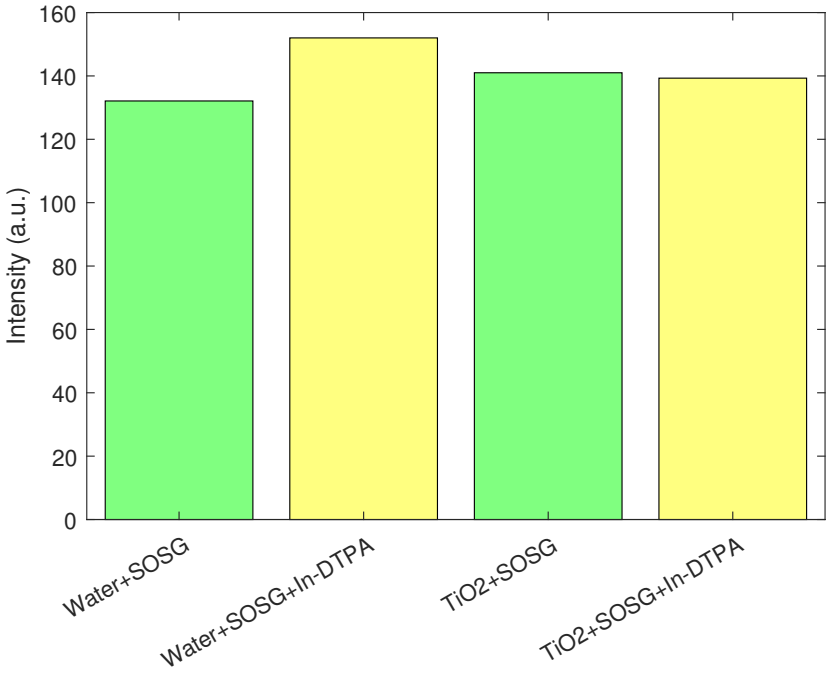

Figure 4.8: The fluorescence of SOSG for samples containing MilliQ water and TiO_2 (0.5 g/L) in the presence and absence of ^{111}In-DTPA for 1h of radiation time. n=1

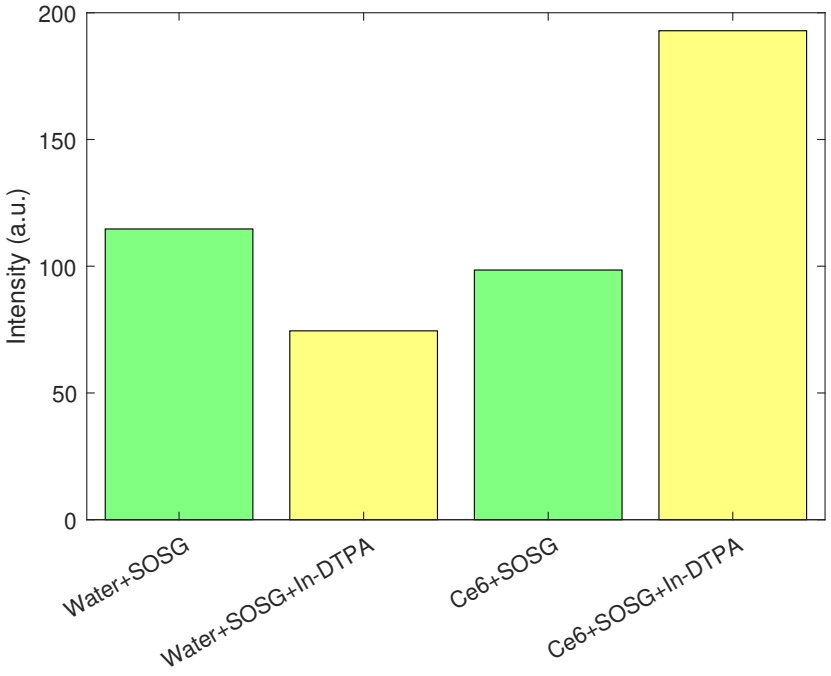

Figure 4.9: The fluorescence of SOSG for samples containing MilliQ water and Ce6 (6 μg/mL) in the presence and absence of ^{111}In-DTPA for 1h of radiation time. n=1

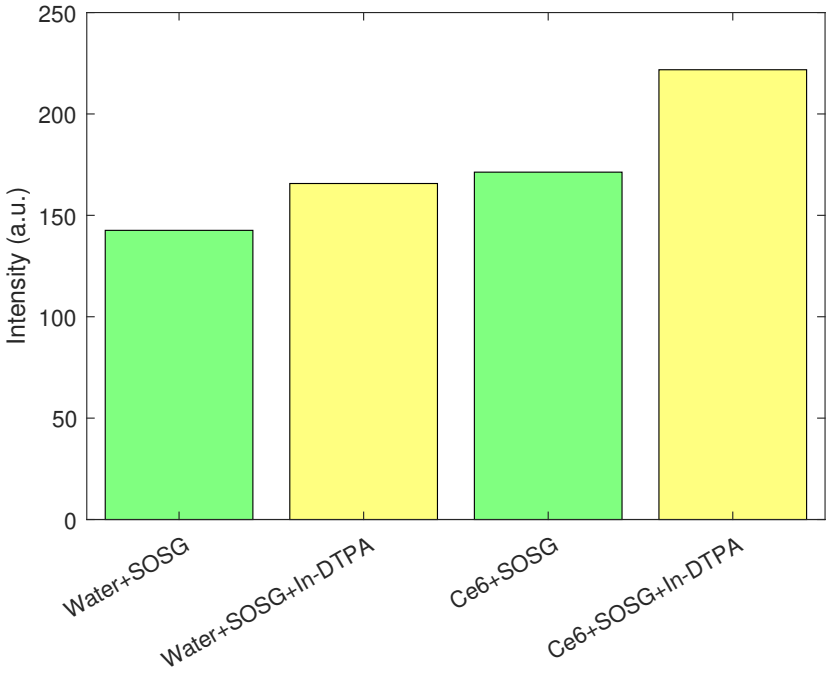

Figure 4.10: The fluorescence of SOSG for samples containing MilliQ water and Ce6 (6 μg/mL) in the presence and absence of ^{111}In-DTPA for 24h of radiation time. n=1

Figures 4.8, 4.9 and 4.10 show the fluorescence intensity of ^{111}In-DTPA samples. The results were positive, as samples which contained ^{111}In radionuclides had higher fluorescence intensities. The experiment was repeated. The results are shown in figure 4.11.

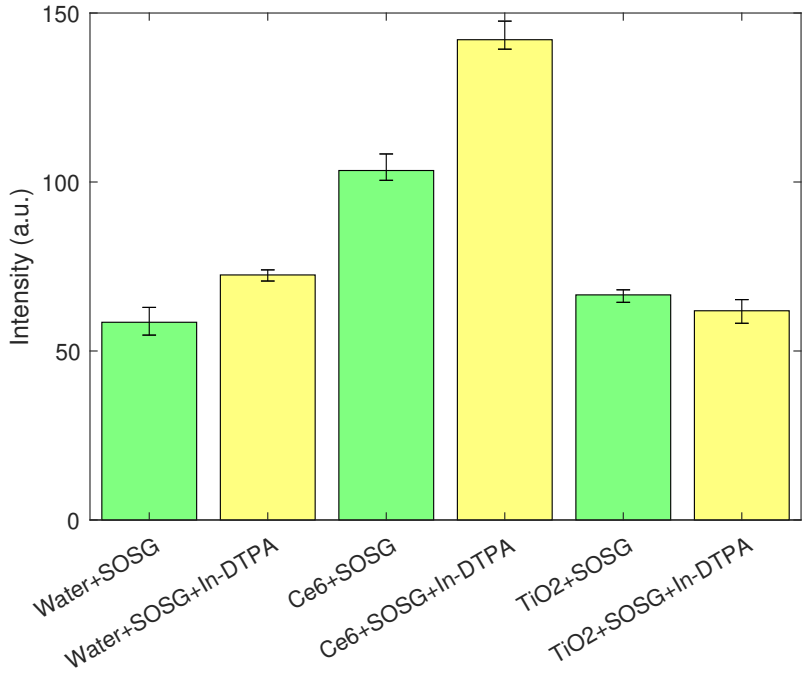

Figure 4.11: The fluorescence of SOSG for samples containing MilliQ water, TiO_2 (0.5 g/L) and Ce6 (6 μg/mL) in the presence and absence of ^{111}In-DTPA for 1h of radiation time. The error bars represent the experimental uncertainty. n=3

4.1.3. Yttrium-90

As third source of radiation, different foils of yttrium-90 which had different activities were used.

In this specific experiment, only one sample was prepared for the groups that were not irradiated by ^{90}Y (this is represented in figure 4.12 with no error bars), the group irradiated by ^{90}Y was prepared and analyzed three times. The foil used in this experiment had an activity of 12.26 MBq at the start of the experiment.

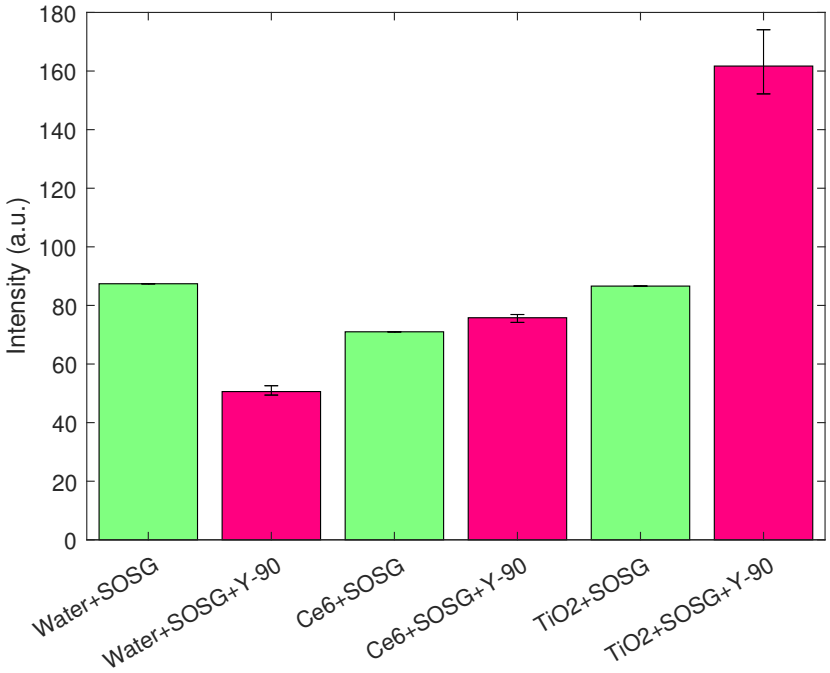

Figure 4.12: The fluorescence of SOSG for samples containing MilliQ water, TiO_2 (0.5 g/L) and Ce6 (6 μg/mL) in the presence and absence of ^{90}Y for 1.5h of radiation time. The error bars represent the experimental uncertainty. At the start of the experiment, the samples in the first red bar had an average dose rate of 0.15 Gy/h, the second 0.18 Gy/h and the third 0.17 Gy/h. n=3

These samples were analyzed again after 4 days. The TiO_2 was only prepared once and could not be reused after being centrifuged for the 1.5h measurement.

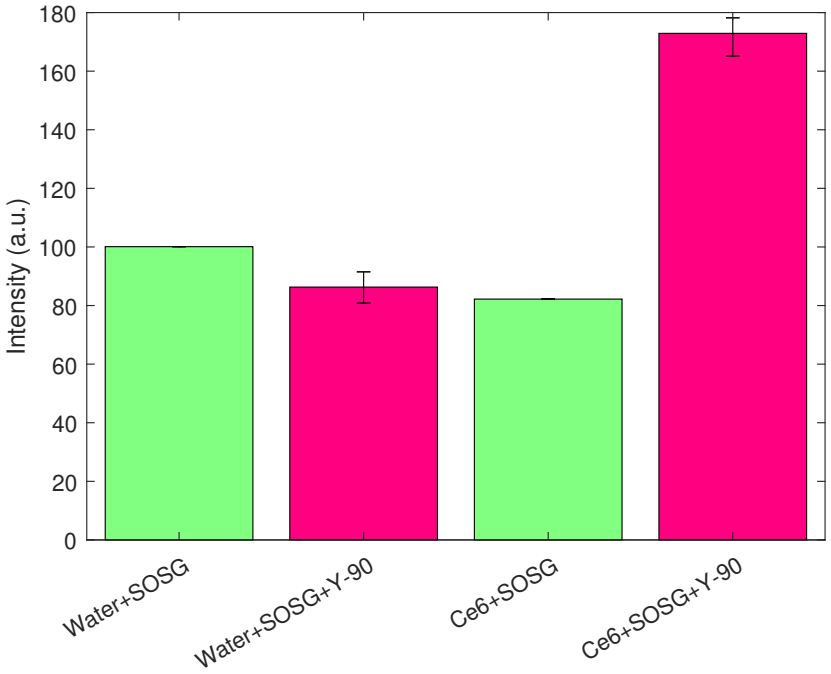

Figure 4.13: The fluorescence of SOSG for samples containing MilliQ water, TiO_2 (0.5 g/L) and Ce6 (6 μg/mL) in the presence and absence of ^{90}Y for 96h of radiation time. The error bars represent the experimental uncertainty. At the start of the experiment, the samples in the first red bar had an average dose rate of 0.15 Gy/h and the second 0.18 Gy/h. n=3

The following results (figures 4.14 and 4.15) show samples that were put onto a foil with an activity of 34.2 MBq.

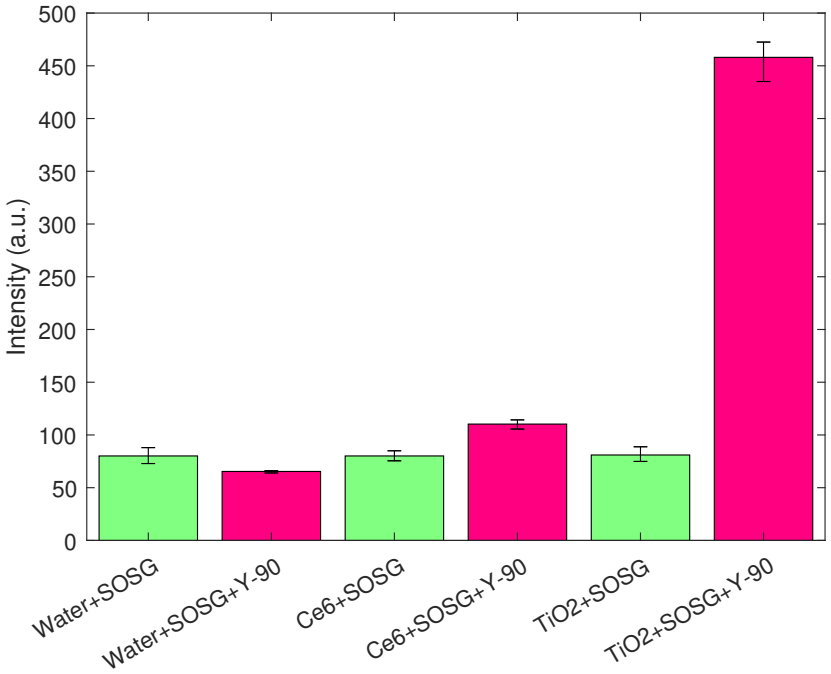

Figure 4.14: The fluorescence of SOSG for samples containing MilliQ water, TiO_2 (0.5 g/L) and Ce6 (6 μg/mL) in the presence and absence of ^{90}Y for 2h of radiation time. The error bars represent the experimental uncertainty. At the start of the experiment, the samples in the first red bar had an average dose rate of 0.31 Gy/h, the second 0.29 Gy/h and the third 0.30 Gy/h. n=3

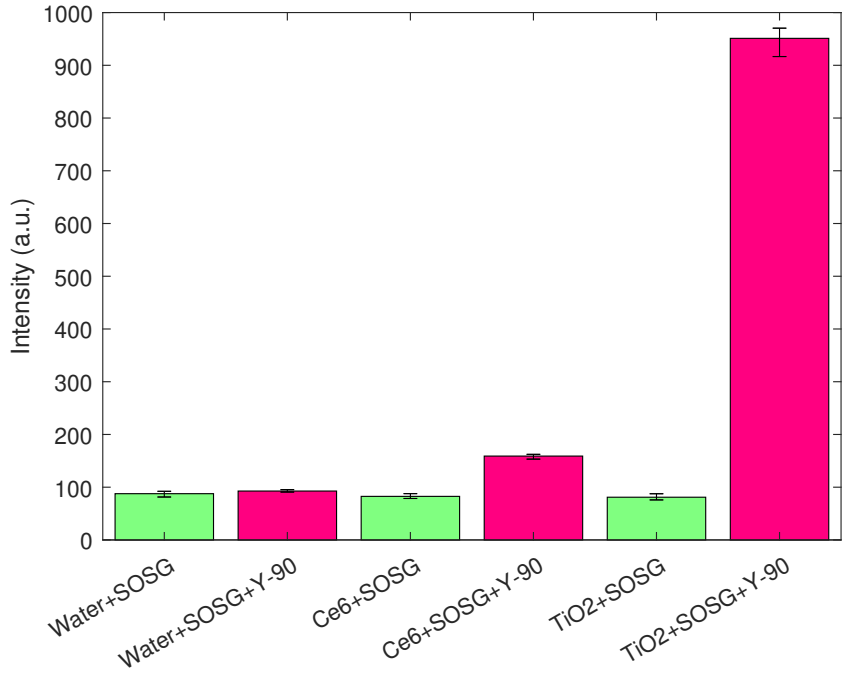

Figure 4.15: The fluorescence of SOSG for samples containing MilliQ water, TiO_2 (0.5 g/L) and Ce6 (6 μg/mL) in the presence and absence of ^{90}Y for 24h of radiation time. The error bars represent the experimental uncertainty. At the start of the experiment, the samples in the first red bar had an average dose rate of 0.31 Gy/h, the second 0.29 Gy/h and the third 0.30 Gy/h. n=3

The following results (figures 4.16 and 4.17) show samples that were put onto a foil with an activity of 96.5 MBq.

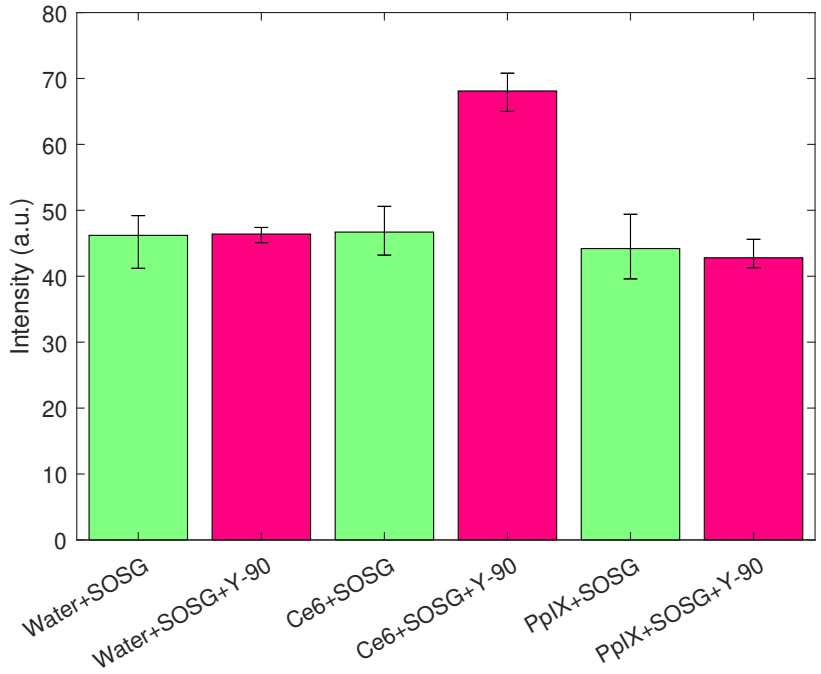

Figure 4.16: The fluorescence of SOSG for samples containing MilliQ water, TiO_2 (0.5 g/L) and Ce6 (6 μg/mL) in the presence and absence of ^{90}Y for 1h of radiation time. The error bars represent the experimental uncertainty. At the start of the experiment, the samples in the first red bar had an average dose rate of 0.86 Gy/h, the second 0.81 Gy/h and the third 0.85 Gy/h. n=3

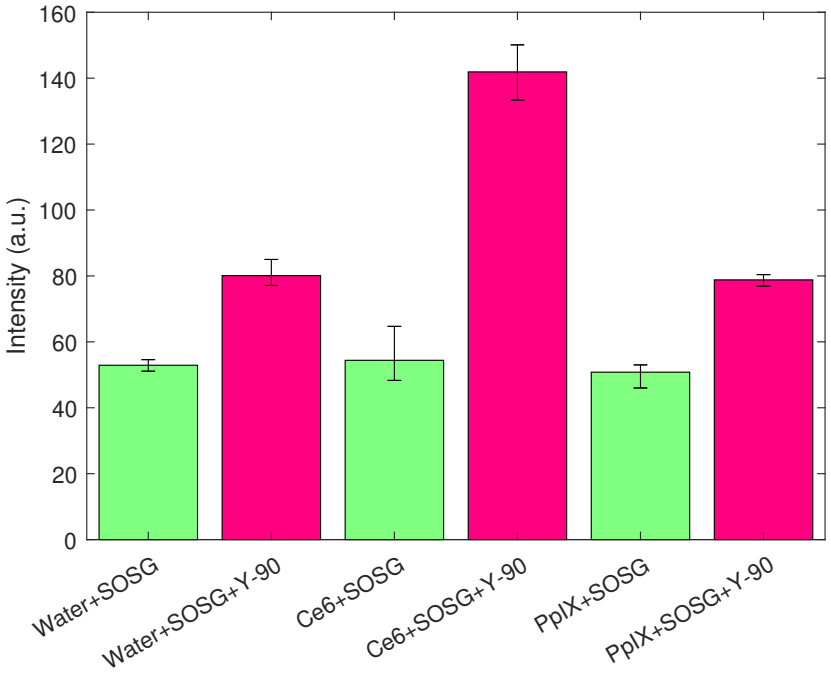

Figure 4.17: The fluorescence of SOSG for samples containing MilliQ water, TiO_2 (0.5 g/L) and Ce6 (6 μg/mL) in the presence and absence of ^{90}Y for 24h of radiation time. The error bars represent the experimental uncertainty. At the start of the experiment, the samples in the first red bar had an average dose rate of 0.86 Gy/h, the second 0.81 Gy/h and the third 0.85 Gy/h. n=3

The following results (figures 4.18 and 4.19) show samples that were put onto a foil with an activity of 157 MBq.

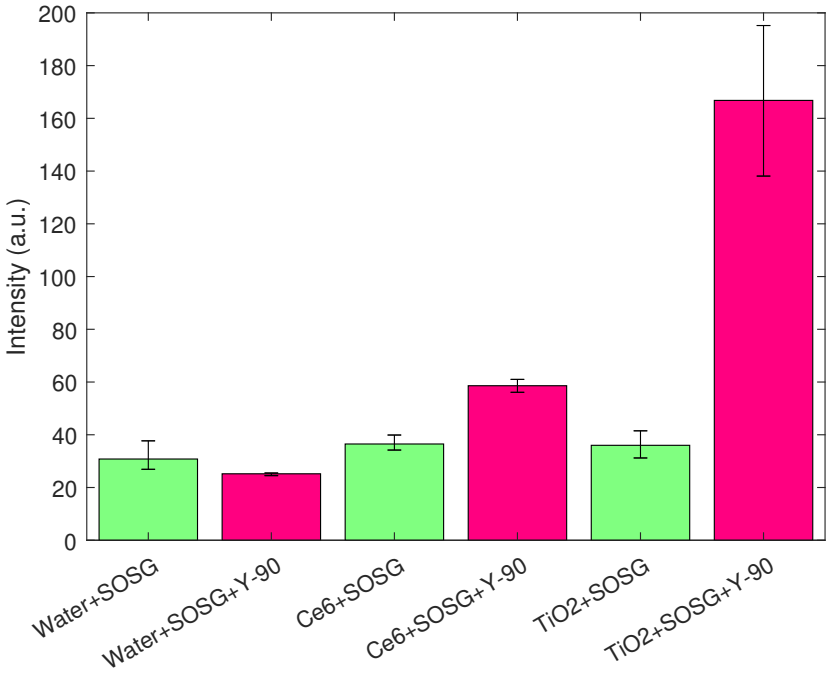

Figure 4.18: The fluorescence of SOSG for samples containing MilliQ water, TiO_2 (0.5 g/L) and Ce6 (6 μg/mL) in the presence and absence of ^{90}Y for 1.5h of radiation time. The error bars represent the experimental uncertainty. At the start of the experiment, the samples in the first red bar had an average dose rate of 0.96 Gy/h, the second 1.08 Gy/h and the third 1.05 Gy/h. n=3

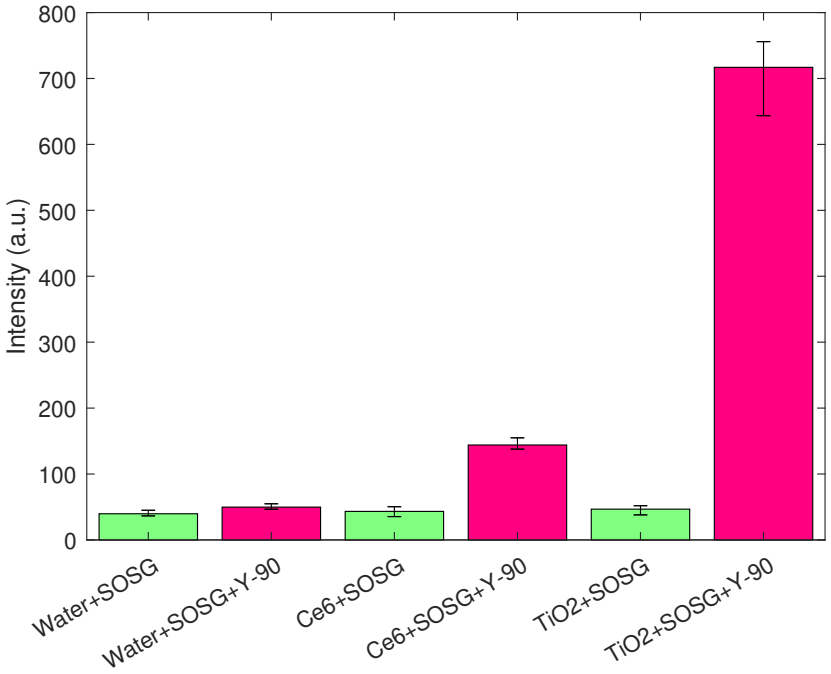

Figure 4.19: The fluorescence of SOSG for samples containing MilliQ water, TiO_2 (0.5 g/L) and Ce6 (6 μg/mL) in the presence and absence of ^{90}Y for 24h of radiation time. The error bars represent the experimental uncertainty. At the start of the experiment, the samples in the first red bar had an average dose rate of 0.96 Gy/h, the second 1.08 Gy/h and the third 0.91 Gy/h. n=3

5

Discussion

5.1. $^1\mathbf{O}_2$ formation

5.1.1. Precipitation phenomenon

It is important to notice the different sources of radiation. In this thesis, three sources of radiation have been used. These are: ^{177}Lu,^{111}In and ^{90}Y. As was explained in the chapter 2, the theory chapter, ^{177}Lu decays by β^- emission and γ emission, ^{111}In decays by electron capture (EC) which involves the emission of X-rays, and ^{90}Y decays by β^- emission.

Initial experiments with ^{177}Lu and ^{111}In in the presence of TiO_2 and Ce6 showed that there is a decrease in fluorescence intensity of SOSG, in comparison to controls. This phenomenon was thought to occur due to the formation of precipitates, i.e. small nano-particles of Indium(III) hydroxide, $In(OH)_3$ and Lutetium(III) hydroxide, $Lu(OH)_3$ which may cause the SOSG molecule adsorption to their surface leading to loss of signal.

This was checked by chelating ^{111}In radionuclides so that they do not precipitate. Indeed, chelation between indium and DTPA seemed to remove the phenomenon of the decrease in fluorescence intensity of SOSG.

Now that we know that chelation with DTPA solves the lower than expected signal intensity, the focus can shift to the production of singlet oxygen by photosensitizers and photocatalysts.

5.1.2. Effect of ionizing radiation on TiO_2

Initial experiments with ^{111}In-DTPA in TiO_2 solution were not that promising. In fact, ^{111}In-DTPA in TiO_2 solution showed no increase in fluorescence intensity at all. This may be because the X-rays from ^{111}In decay do not carry a high enough energy to activate TiO_2 resulting in no increase in fluorescence intensity. However, this is still speculation.

Experiments with yttrium-90 showed a completely different picture in terms of fluorescence intensity increase for TiO_2. Activities varying from 12.3 MBq to 157 Mbq all showed significant increase for TiO_2 in fluorescene intensity.

5.1.3. Effect of ionizing radiation on Ce6 and PpIX

In contrast to initial experiments with ^{111}In-DTPA in TiO_2 solution, the fluorescence intensity of ^{111}In-DTPA in Chlorin e6 solution showed an increase.

Similar to TiO_2, an increase in fluorescence activity was seen for Ce6 in presence of yttrium-90. However, this increase was not as much as that of TiO_2. This trend was clear for all activities tested.

PpIX was only tested with an activity of 96.5 MBq. PpIX showed an almost identical signal intensity to water for multiple radiation times. This could mean that PpIX does not get activated as a photosensitizer in presence of beta radiation at all. However, this conclusion is premature, as during these experiments PpIX was tried to be dissolved into water. PpIX seemed to be almost insoluble in water. To determine the potential of PpIX as a photosensitizer, PpIX should be properly dissolved first and then tested again.

5.2. Possible photosensitization mechanism

The difference between TiO_2 and Ce6 could give a clue to a possible mechanism behind the photosensitization of Ce6. Chlorin e6 seems to be activated by X-rays while TiO_2 does not seem to be activated by those same X-rays. Both Ce6 and TiO_2 seem to be activated by high energy beta-minus emission.

Photosensitizers are excited to high-energy states after absorbing excitation photons and this energy can be dissipated through intersystem crossing (ISC) which in turn leads to a cascade forming reactive oxygen species. Chlorin e6 is a tetrapyrrole-based photosensitizer [37], while TiO_2 is a heavy metal based photocatalyst. How ROS are produced by both photosensitizers and photocatalysts were explained in the theory.

The possible mechanism behind the photosensitization of Ce6 could be that both low and high energy radiation have sufficient energy to excite ground-state photosensitizers to a high-energy state, resulting in dissipation of energy through ISC and the resulting cascade of forming ROS.

However, for TiO_2, low energy X-rays do not excite enough electrons to result in many surface interactions of charge carriers with adsorbed molecules or to result in formation of excitons. In turn, this leads to virtually no formation of ROS. This could explain why Chlorin e6 seems to be activated by low energy X-rays while TiO_2 does not seem to be activated by those same X-rays.

Furthermore, this can also explain why the fluorescence intensity increase of Ce6 was not as much as that of TiO_2 in presence of yttrium-90. It could be that low and high energies have the same excitation effect to excite ground-state photosensitizers to a high-energy state, regardless of how high the energies are, as long as they are high enough to excite photosensitizers.

For TiO_2, this could be different in the way that much higher energies lead to much more electrons being excited, resulting in many surface interactions of charge carriers with adsorbed molecules. In turn, this leads to more ROS production.

5.3. Applicability in medicine

Photosensitizers, like Ce6 and TiO_2, need to enter the body and they need to be irradiated to produce reactive oxygen species. For this, both the photosensitizer and the radiation source would need to be encapsulated in a kind of micelle to be injected in the body, the micelle needs to be able to enter a cell and the micelle needs to be broken down for the contents to be released. Only then, would the production of ROS by the photosensitizer have any use for therapy.

To realize this, many factors need to be researched and be accounted for. Examples are: pH of different tissues, the permeability and retention of micelles, the release of drugs into the cell. These aspects go beyond the scope of this thesis.

Regarding whether Ce6 or TiO_2 can be used in combination with ionizing radiation in medicine is not clear. Not only should other sources of radiation be tested together with these photosensitizers, another chelator should be tested, as DTPA is not cell membrane permeable.

6

Conclusion

6.1. Effect of ionizing radiation on Ce6 and TiO_2

The goal of this thesis was to study the effect of ionizing radiation on the generation of singlet oxygen when using photosensitizers (Ce6, PpIX) and phototocatalysts (TiO_2). The ability of both TiO_2 and Ce6 to produce singlet oxygen were analyzed. The results under irradiation by different radiation sources were compared. For the detection of singlet oxygen fluorescence spectrometry was used. The radiation sources were ^{177}Lu,^{111}In and ^{90}Y.

Based on the results, the following conclusions can be drawn:

- Both Ce6 and TiO_2 generate singlet oxygen when irradiated by ionizing radiation.
- Ce6 gets activated by both low energy X-rays and high energy beta-minus emission.
- TiO_2 gets activated by high energy beta-minus emission, but not by low energy X-rays.

References

[1] cbs.nl. *Overledenen; doodsoorzaak, kwartaal en jaar overlijden*. 2023. URL: https://www.cbs.nl/nl-nl/cijfers/detail/82899NED# (visited on 05/19/2023).

[2] National Cancer Institute. *Types of Cancer treatment*. 2023. URL: https://www.cancer.gov/about-cancer/treatment/types (visited on 05/19/2023).

[3] National Cancer Institute. *radiotherapy*. 2023. URL: https://www.cancer.gov/publications/dictionaries/cancer-terms/def/radiotherapy (visited on 06/04/2023).

[4] National Cancer Institute. *Photodynamic therapy*. 2023. URL: https://www.cancer.gov/about-cancer/treatment/types/photodynamic-therapy (visited on 05/23/2023).

[5] National Cancer Institute. *neoplasm*. 2023. URL: https://www.cancer.gov/publications/dictionaries/cancer-terms/def/neoplasm (visited on 05/19/2023).

[6] Center for Disease Control and Prevention. *What is Radiation?* 2023. URL: https://www.cdc.gov/nceh/radiation/what_is.html (visited on 05/21/2023).

[7] United Stated Environmental Protection Agency. *radiation sources and doses*. 2023. URL: https://www.epa.gov/radiation/radiation-sources-and-doses (visited on 05/22/2023).

[8] M. Luntz, A. Mozumder, and A.C. Upton. *radiation physics*. 2023. URL: https://www.britannica.com/science/radiation (visited on 05/21/2023).

[9] A. Galindo. *What is radiation?* 2023. URL: https://www.iaea.org/newscenter/news/what-is-radiation (visited on 05/21/2023).

[10] S.B. McGrayne, J. Trefil, and G.F. Bertsch. *atom*. 2023. URL: https://www.britannica.com/science/atom (visited on 05/22/2023).

[11] E.P. Steinberg and J.O. Rasmussen. *radioactivity*. 2023. URL: https://www.britannica.com/science/radioactivity (visited on 05/22/2023).

[12] The Editors of Encyclopaedia Brittanica. *radioactive isotope*. 2023. URL: https://www.britannica.com/science/radioactive-isotope (visited on 05/22/2023).

[13] Australian Radiation Protection and Nuclear Safety Agency. *alpha particles*. 2023. URL: https://www.arpansa.gov.au/understanding-radiation/what-is-radiation/ionising-radiation/alpha-particles (visited on 06/02/2023).

[14] D. Ilem-Ozdemir et al. *Biomedical Applications of Nanoparticles*. 1st ed. pp. 457-490. Bucharest, Romania: Elsevier, 2019.

[15] Harvard Natural Sciences Lecture Demonstrations. *α, β, γ Penetration and Shielding*. 2023. URL: https://sciencedemonstrations.fas.harvard.edu/presentations/%CE%B1-%CE%B2-%CE%B3-penetration-and-shielding (visited on 06/04/2023).

[16] Sam Brind. *What Is Nuclear Radiation?* 2023. URL: https://owlcation.com/stem/What-is-Nuclear-Radiation (visited on 06/12/2023).

[17] Western Oregon University. *Radioactivity and Nuclear Chemistry*. 2023. URL: https://wou.edu/chemistry/courses/online-chemistry-textbooks/ch103-allied-health-chemistry/ch103-chapter-3-radioactivity/ (visited on 06/12/2023).

[18] Wizeprep. *Beta Decay : Electron Capture*. 2023. URL: https://www.wizeprep.com/online-courses/22043/chapter/8/core/3/4 (visited on 06/12/2023).

[19] Encyclopaedia Brittanica. *yttrium*. 2023. URL: https://www.britannica.com/science/yttrium (visited on 05/23/2023).

[20] T. Wu, H. Chiu, and N. L. Ignjatović. *Nanotechnologies in Preventive and Regenerative Medicine*. 1st ed. Champaign, Illinois (United States): Elsevier, 2018.

[21] NRG Advancing Nuclear Medicine. *yttrium-90*. 2023. URL: https://www.advancingnuclearmedicine.com/products/yttrium-90 (visited on 05/23/2023).

[22] Encyclopaedia Brittanica. *indium*. 2023. URL: https://www.britannica.com/science/indium (visited on 05/23/2023).

[23] National Nuclear Data Center. *Decay Radiation indium-111*. 2023. URL: https://www.nndc.bnl.gov/nudat3/DecayRadiationServlet?nuc=111In&unc=NDS (visited on 06/02/2023).

[24] Encyclopaedia Brittanica. *lutetium*. 2023. URL: https://www.britannica.com/science/lutetium (visited on 05/23/2023).

[25] National Nuclear Data Center. *Decay Radiation lutetium-177*. 2023. URL: https://www.nndc.bnl.gov/nudat3/DecayRadiationServlet?nuc=177Lu&unc=NDS (visited on 06/02/2023).

[26] Center for Disease Control and Prevention. *Radiation in Healthcare: Nuclear Medicine*. 2023. URL: https://www.cdc.gov/nceh/radiation/nuclear_medicine.htm#:~:text=Nuclear%20medicine%20uses%20radioactive%20material,or%20tissue%20(for%20treatment). (visited on 06/12/2023).

[27] T. Herron and W. Gossman. *111 Indium White Blood Cell Scan*. 2023. URL: https://www.ncbi.nlm.nih.gov/books/NBK554556/ (visited on 06/12/2023).

[28] Cancer Quest. *Advantages and Disadvantages of Radiation Therapy*. 2023. URL: https://www.cancerquest.org/patients/treatments/radiation-therapy#toc-advantages-iIwIA-Qd (visited on 06/05/2023).

[29] J. H. Correia et al. "Photodynamic Therapy Review: Principles, Photosensitizers, Applications, and Future Directions". In: *Pharmaceutics* 13.9 (2021), p. 1332.

[30] X. Wu and C. Dong. *Photonanotechnology for Therapeutics and Imaging*. 1st ed. Michigan, United States: Elsevier, 2020.

[31] IUPAC Gold Book. *photosensitization*. 2023. URL: https://goldbook.iupac.org/terms/view/P04652 (visited on 06/12/2023).

[32] IUPAC Gold Book. *photosensitization*. 2023. URL: https://goldbook.iupac.org/terms/view/P04580 (visited on 06/12/2023).

[33] National Cancer Institute. *reactive oxygen species*. 2023. URL: https://www.cancer.gov/publications/dictionaries/cancer-terms/def/reactive-oxygen-species (visited on 05/23/2023).

[34] M. Redza-Dutordoir and D.A. Averill-Bates. "Activation of apoptosis signalling pathways by reactive oxygen species". In: *Biochimica et Biophysica Acta (BBA)* 1863.12 (2016), pp. 2977–2992.

[35] A. Manivannan, P. Soundarajan, and B.R. Jeong. *Reactive Oxygen Species in Plants: Boon Or Bane Revisiting the Role of ROS*. 1st ed. pp. 319-329. Chhattisgarh, India: John Wiley and Sons Ltd., 2017.

[36] M.R. Hamblin and Y. Huang. *Imaging in Photodynamic Therapy*. Boca Raton, FL, USA: Taylor and Francis Group, 2017.

[37] Y. Xiong, X. Tian, and H.W. Ai. "Molecular Tools to Generate Reactive Oxygen Species in Biological Systems". In: *Bioconjugate chemistry* 30.5 (2019), pp. 1297–1303.

[38] R. van den Elshout. "Analysis of the ability of titanium dioxide nanoparticles to produce singlet oxygen and hydrogen peroxide under ionising radiation". Available at http://repository.tudelft.nl/.. Bachelor's thesis. Delft, the Netherlands: University of Technology Delft, July 2022.

[39] Y. Nosaka and A.Y. Nosaka. "Generation and Detection of Reactive Oxygen Species in Photocatalysis". In: *Chemical reviews* 117.17 (2017), pp. 11302–11336.

[40] Fisher scientific. *Invitrogen™ Singlet Oxygen Sensor Green*. 2023. URL: https://www.fishersci.com/shop/products/molecular-probes-singlet-oxygen-sensor-green-special-packaging/S36002 (visited on 05/24/2023).

[41] S. Kim, M. Fujitsuka, and T. Majima. "Photochemistry of Singlet Oxygen Sensor Green". In: *The Journal of Physical Chemistry B* 117.45 (2013), pp. 13985–13992.

[42] H. Liu et al. “Singlet Oxygen Sensor Green is not a Suitable Probe for $^1O_2$ in the Presence of Ionizing Radiation”. In: *Scientific Reports* 9 (2019).

[43] Moravek Inc. *What Exactly Is Radiolabeling?* 2023. URL: https://www.moravek.com/what-exactly-is-radiolabeling/ (visited on 06/05/2023).

[44] Chemical Dictionary. *chelation definition*. 2023. URL: https://www.chemicool.com/definition/chelation.html (visited on 06/05/2023).

[45] Centers for Disease Control and Prevention. *DTPA (Diethylenetriamine pentaacetate)*. 2023. URL: https://www.cdc.gov/nceh/radiation/emergencies/dtpa.htm (visited on 06/05/2023).

[46] Mitopedia. *DTPA*. 2023. URL: https://www.bioblast.at/index.php/DTPA (visited on 06/05/2023).

[47] via Wikimedia Commons NEUROtiker Public domain. *DTPA*. 2023. URL: https://upload.wikimedia.org/wikipedia/commons/5/50/Diethylentriaminpentaessigs%C3%A4ure.svg (visited on 06/05/2023).

[48] H. Honarvar et al. “Evaluation of HER2-specific peptide ligand for its employment as radiolabeled imaging probe”. In: *Scientific Reports* 8 (2018).

[49] National Center for Biotechnology Information. *PubChem Compound Summary for CID 5479494, Chlorin e6*. 2023. URL: https://pubchem.ncbi.nlm.nih.gov/compound/Chlorin-e6 (visited on 06/13/2023).

[50] Sigma Aldrich. *Buffer Reference center*. 2023. URL: https://www.sigmaaldrich.com/NL/en/technical-documents/protocol/protein-biology/protein-concentration-and-buffer-exchange/buffer-reference-center#sodiumacetate (visited on 05/28/2023).

[51] S. Devic. “Radiochromic film dosimetry: past, present, and future”. In: *Physica Medica* 27.3 (2011), pp. 122–134.

[52] Schindelin J et al. “Fiji: an open-source platform for biological-image analysis”. In: *Nature Methods* 9.7 (2012), pp. 676–682.

[53] M.M Vora. “HPLC analysis of indium-111 diethylenetriaminepentaacetic acid (^{111}In-DTPA) radiopharmaceutical”. In: *International Journal of Radiation Applications and Instrumentation. Part A. Applied Radiation and Isotopes* 42.1 (1990), pp. 19–24.

[54] The MathWorks Inc. *MATLAB version: 9.9.0.1570001 (R2020b*. Natick, Massachusetts, United States, 2023. URL: https://www.mathworks.com.

A

MATLAB code

The following code can be used to visualize a bar graph.

```
"""
In X, the label of each sample should be given. In Y, the values of signal intensity are put in.
b.CData(1,:) = [0.5 1 0.5] determines the color in RGB code.
"""
X = categorical({'Water+SOSG','Water+SOSG+In-111','TiO2+SOSG','TiO2+SOSG+In-111','Ce6+SOSG','Ce6+SOSG+In-111'});
X = reordercats(X,{'Water+SOSG','Water+SOSG+In-111','TiO2+SOSG','TiO2+SOSG+In-111','Ce6+SOSG','Ce6+SOSG+In-111'});
Y = [data1 data2 ... data6];
b = bar(X,Y);
b.FaceColor = 'flat';
b.CData(1,:) = [0.5 1 0.5];
b.CData(2,:) = [0 0 1];
b.CData(3,:) = [0.5 1 0.5];
b.CData(4,:) = [0 0 1];
b.CData(5,:) = [0.5 1 0.5];
b.CData(6,:) = [0 0 1];
```

The following code can be used to visualize a bar graph with error bars.

```
"""
In X, the label of each sample should be given. In Y, the values of signal intensity are put in.
b.CData(1,:) = [0.5 1 0.5] determines the color in RGB code.
The upper and lower error limit should be filled into errhigh and errlow respectively.
"""
X = categorical({'Water+SOSG','Water+SOSG+Y-90','Ce6+SOSG','Ce6+SOSG+Y-90','TiO2+SOSG','TiO2+SOSG+Y-90'});
X = reordercats(X,{'Water+SOSG','Water+SOSG+Y-90','Ce6+SOSG','Ce6+SOSG+Y-90','TiO2+SOSG','TiO2+SOSG+Y-90'});
data = [data1 data2 ... data6]';
errhigh = [error1 error2 ... error 6];
errlow  = [error1 error2 ... error 6];

b = bar(X,data);
b.FaceColor = 'flat';
b.CData(1,:) = [0.5 1 0.5];
b.CData(2,:) = [1 0 0.5];
b.CData(3,:) = [0.5 1 0.5];
b.CData(4,:) = [1 0 0.5];
b.CData(5,:) = [0.5 1 0.5];
b.CData(6,:) = [1 0 0.5];

hold on
er = errorbar(X,data,errlow,errhigh);
er.Color = [0 0 0];
er.LineStyle = 'none';
hold off
```

B

Chelation results

Given below are the chelation results for each chelation experiment

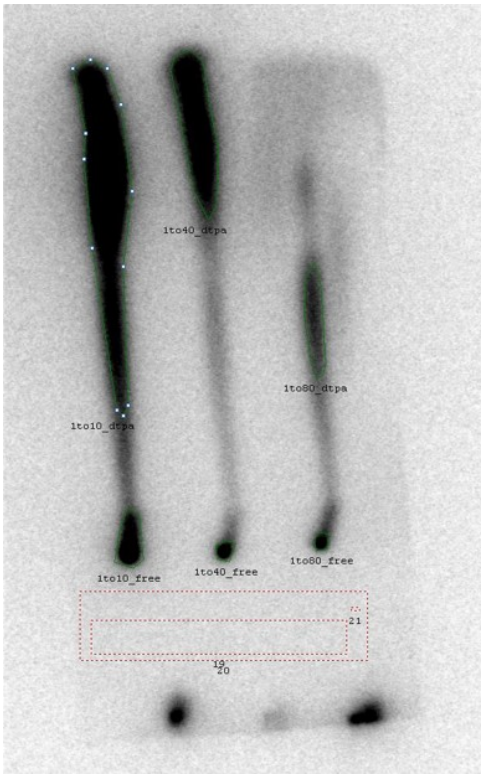

Figure B.1: Result of ”Different solvent, mobile phase and DTPA concentration” experiment. The left TLC is the result of a 1:10 ^{111}In:DTPA ratio, the middle 1:40 ^{111}In:DTPA ratio and the right 1:80 ^{111}In:DTPA ratio.

For figure B.1:

- For 1:10 ^{111}In:DTPA ratio, 91 percent of indium-111 was chelated.
- For 1:40 ^{111}In:DTPA ratio, 94 percent of indium-111 was chelated.
- For 1:80 ^{111}In:DTPA ratio, 84 percent of indium-111 was chelated.

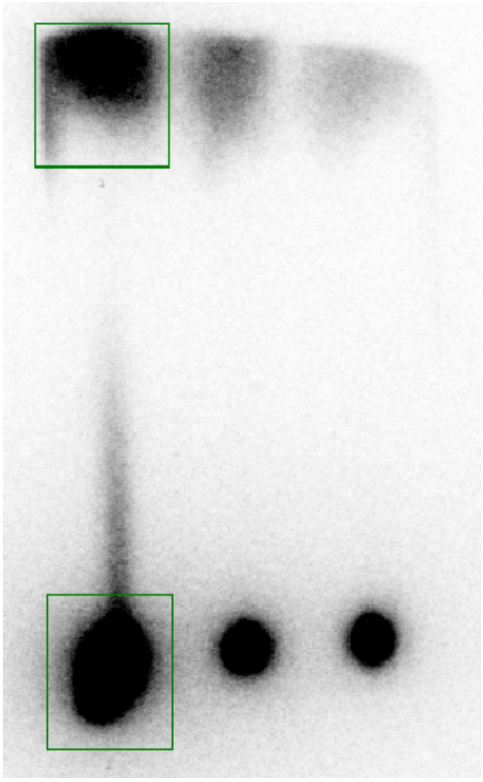

Figure B.2: Result of ”Different pH” with pH = 7.7 experiment. The left TLC is the result of a 1:10 ^{111}In:DTPA ratio, the middle 1:40 ^{111}In:DTPA ratio and the right 1:80 ^{111}In:DTPA ratio.

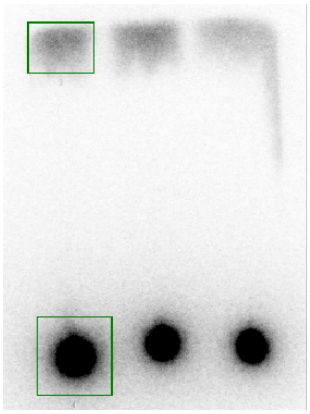

Figure B.3: Result of ”Different pH” with pH = 5.6 experiment. The left TLC is the result of a 1:10 ^{111}In:DTPA ratio, the middle 1:40 ^{111}In:DTPA ratio and the right 1:80 ^{111}In:DTPA ratio.

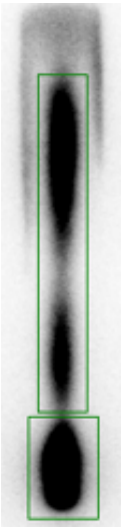

Figure B.4: Result of ”Different mixing time periods” with t = 30 min experiment.

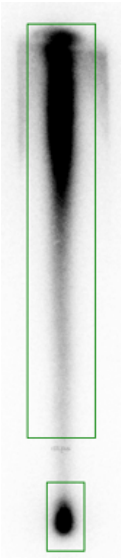

Figure B.5: Result of ”Different mixing time periods” with t = 1h experiment.

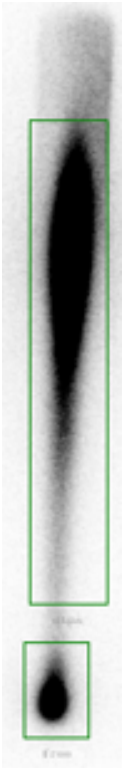

Figure B.6: Result of ”Different mixing time periods” with t = 3h experiment.

Figure B.7: Result of ”Higher DTPA concentration: 1.0 μM” experiment.

Figure B.8: Result of chelation experiment for figures 4.9 and 4.10.

Figure B.9: Result of chelation experiment for figure 4.11.